ACCSCIENCE PUBLISHING

International Journal of Bioprinting

REVIEW ARTICLE

Advanced three-dimensional bioprinting for *in vitro* tumor model engineering: From biomimetic model construction to personalized precision medicine

Zhiyan Zhang[1†], Tingyu Wang[2†], Bo Qiao[3], Xiangran Cui[4*], Shuo Wu[5*], and Guoliang Zheng[3*]

[1]First Department of Radiotherapy, The Fifth People's Hospital of Shenyang, Shenyang, Liaoning, China

[2]Department of Laboratory Medicine, The First Hospital of China Medical University, Shenyang, Liaoning, China

[3]Department of Gastric Surgery, Cancer Hospital of Dalian University of Technology, Liaoning Cancer Hospital & Institute, Shenyang, Liaoning, China

[4]Department of Orthopedics, Second Affiliated Hospital of Liaoning University of Traditional Chinese Medicine, Shenyang, Liaoning, China

[5]Department of Blood Diseases and Breast Medicine, Cancer Hospital of Dalian University of Technology, Liaoning Cancer Hospital & Institute, Shenyang, Liaoning, China

[†]*These authors contributed equally to this work.*

***Corresponding authors:**
Xiangran Cui (1334367621@qq.com);
Shuo Wu (toutoushu@126.com);
Guoliang Zheng (zhengboren1@126.com)

Citation: Zhang Z, Wang T, Qiao B, Cui X, Wu S, Zheng G. Advanced three-dimensional bioprinting for *in vitro* tumor model engineering: From biomimetic model construction to personalized precision medicine. *Int J Bioprint*. doi: 10.36922/IJB026400430

Received: October 2, 2026

Revised: October 26, 2026

Accepted: November 2, 2026

Published online: November 19, 2026

Copyright: © 2026 Author(s). This is an Open-Access article distributed under the terms of the Creative Commons Attribution License, permitting distribution, and reproduction in any medium, provided the original work is properly cited.

Publisher's Note: AccScience Publishing remains neutral with regard to jurisdictional claims in published maps and institutional affiliations.

Abstract

Three-dimensional (3D) bioprinting technology offers a transformative approach for constructing biomimetic tumor organoid models that overcome the limitations of traditional two-dimensional cell cultures and animal models. This review systematically summarizes recent advances in 3D bioprinted tumor organoids, emphasizing extrusion-based, inkjet-based, and lithography-based bioprinting methods. These technologies enable precise spatial control of cell distribution and tissue architecture, achieving high reproducibility while maintaining complex tumor microenvironmental characteristics. Applications across multiple cancer types—including colorectal, gastric, pancreatic, breast, glioma, renal, bladder, lung, and thyroid cancers—demonstrate significant potential for drug screening, tumor heterogeneity research, and preclinical evaluation of individualized treatment responses. Despite substantial progress, challenges remain regarding multicellular complexity simulation, technical resolution, and biomaterial optimization. Future directions include integrating four-dimensional bioprinting, multiomics analysis, and immune microenvironment reconstruction to enhance physiological fidelity and clinical applicability, ultimately advancing precision oncology and personalized cancer treatment strategies.

Keywords: Biomaterials; Tumor organoids; Three-dimensional bioprinting; Personalized medicine; Tumor microenvironment

1. Introduction

As a major global public health challenge, cancer imposes a heavy burden on human health and the social economy due to its high incidence and mortality rates.[1-3] According to the latest epidemiological data, global cancer incidence continues to rise, with millions of new cases each year, leading to a significant loss of quality of life or even life itself for many patients.[4,5] Despite significant progress in cancer diagnosis and treatment, the complexity of tumors, especially their inherent heterogeneity (including heterogeneity between cells within a tumor and between individual patients), remains a massive obstacle to clinical treatment.[6-9] The limitations of traditional two-dimensional cell culture models and animal models in simulating the tumor microenvironment, predicting drug responses, and capturing tumor heterogeneity have become increasingly apparent, creating an urgent need for the development of more physiologically relevant *in vitro* models to deeply understand the mechanisms of tumor development and promote the realization of precision medicine.[10-15]

The emergence of three-dimensional (3D) bioprinting technology provides a new approach to solving this problem. 3D bioprinting technology can precisely control the spatial distribution and organizational structure of cells to construct 3D tumor models with biomimetic structures.[16-18] Through bioprinting, researchers can precisely control cell types, cell densities, and biological matrix components, making the constructed tumor models closer to the histological characteristics of tumors *in vivo*.[19-21] The combination of microfluidic technology and 3D bioprinting has further advanced *in vitro* tumor models, enabling high-throughput, automated, and uniform mass production of these models.[22-25] However, most current 3D-printed tumor models focus on single cell types or simple two-cell co-culture systems, and simulations of complex interactions and the dynamic evolution of multiple cell types within the tumor microenvironment remain insufficient.[26,27] Therefore, further optimizing 3D bioprinting systems to construct tumor models that better reflect tumor heterogeneity and microenvironmental complexity still requires in-depth exploration.

Against this backdrop, utilizing 3D bioprinting technology to construct tumor organoid models demonstrates tremendous application potential.[28-30] 3D bioprinted tumor organoids can better preserve the original histological structure and cellular heterogeneity of tumors, and more accurately reproduce the interactions among multiple cell types within the tumor microenvironment.[31-33] Cells in 3D bioprinted tumor organoids exist in 3D space, facing nutrient gradients, oxygen gradients, and concentration gradients of intercellular signaling molecules that are closer to those *in vivo*, thereby more faithfully reflecting the biological behavior of tumor cells in the body.[34-36] Secondly, 3D bioprinted tumor organoids possess highly reproducible and standardized characteristics and can significantly reduce operational variability in model preparation compared with traditional manual construction methods.[37-39] Third, by integrating multiple analytical techniques (including genetic analysis, transcriptomic analysis, and drug screening), 3D bioprinted tumor organoids can provide strong support for advancing personalized treatment and precision medicine, and are promising tools for new drug development, preclinical efficacy evaluation, and mechanistic research into drug resistance.[40-45] However, the direct clinical utility of these models for guiding treatment or surgical decisions remains to be rigorously established through prospective clinical trials with appropriate patient numbers, validation designs, and predictive performance metrics.

For this review, we defined organoid in a restricted sense as patient-derived, self-organizing 3D cultures established from primary tumor tissue or biopsy material that preserve key histological architecture, cellular heterogeneity, and, where applicable, relevant lineage-specific or stem-cell-derived differentiation programs. In contrast, cell-line spheroids are aggregates generated from established cell lines without evidence of self-organization from primary tissue; engineered tumor constructs are designed 3D models built primarily by incorporating predefined cells and matrices to mimic selected tumor features; and assembloids are composite systems formed by combining two or more pre-existing organoid or tissue-like modules. Models were classified as organoids only when the source material was patient-derived or primary-tissue-derived, and the resulting structure showed organoid-like self-organization and tissue-relevant morphologic and functional features, rather than being limited to simple spheroid aggregation or scaffold-based reconstruction.

We searched the Web of Science database using "bioprinting," "tumor," and "organoid" as keywords, and retrieved articles published between 2016 and 2026. We then excluded reviews, conference papers, and other non-article formats. After screening the titles and reading the full texts, we finally selected studies that were closely aligned with our research topic.

This review summarizes recent advances in 3D bioprinting for tumor organoid engineering, emphasizing how different printing modalities, biomaterial systems, and multicellular co-culture strategies improve model fidelity and translational value. We first compare the principles, strengths, and limitations of extrusion-based, inkjet-based, and lithography-based bioprinting. We then

highlight representative applications across major cancer types, focusing on how recent studies have improved tumor microenvironment reconstruction, drug screening performance, and patient-specific response prediction (Table 1). Finally, we discuss the major remaining challenges and future directions needed to move bioprinted tumor organoids toward standardized and clinically actionable precision medicine platforms (Figure 1).

Table 1. Summary of the application of three-dimensional bioprinting *in vitro* tumor model

System	Organ	Species	Cell line	Culture time	Method	Printing parameter	Bioinks	Support bath	Summary	Ref
Digestive system	Colorectal cancer	Human	Caco-2	7 d	Extrusion-based 3D bioprinting	Disc model: diameter 2 mm, height 0.82 mm; extrusion nozzle: 410 μM (0.41 mm) high-precision nozzle; printing equipment: BioX (CELLINK); pressure 8–10 kPa; speed 10 ms	RGD bioink/ GelMA	/	3D bioprinting of Caco-2 colorectal cancer cells in RGD and GelMA bioinks achieved 90% viability, with RGD forming glandular-like structures suitable for drug screening	46
		Human	PDOs	36 h	Acoustic droplet printing	25,000 T, 120 mVpp, period 2 s (after intermittent printing, UV curing for 1 min)	5% GelMA	/	SAW acoustic 3D printing of patient-derived colorectal cancer microtissues with CAFs in GelMA models tumor invasion and drug response for personalized therapy	47
		Human	PDOs	36 h	Surface acoustic wave 3D bioprinting	25,000 T, 120 mVpp, period 2 s (after intermittent printing, UV curing for 1 min)	5% GelMA	/	Acoustic SAW 3D bioprinting constructs patient-derived colorectal tumor and healthy organoids in GelMA for predicting 5-FU drug responses and modeling tumor invasion	19
		Human	SW1222	7 d	Extrusion-based 3D bioprinting	The inner diameter is 0.5 mm; flow rate: peptide 50 μL/min, PBS 25 μL/min, cells 15 μL/min; the hybrid system for 3D printing is: IIFK:IDP = 5:1	IIFK:IDP/ IKVAV	/	Extrusion 3D bioprinting of SW1222 colorectal cancer cells in self-assembling IIFK:IDP peptide hydrogels enables lumen-forming organoid formation	32

(*Contd...*)

Table 1. (*Continued*)

System	Organ	Species	Cell line	Culture time	Method	Printing parameter	Bioinks	Support bath	Summary	Ref
		Human	SW480	7 d	Extrusion-based 3D bioprinting	Printing speed 6 mm/s; extrusion speed:1.599 mm/s; printing platform temperature 10 °C; nozzle temperature 15 °C; layer height 2 mm; filling line distance 0.2 mm	Gelatin/sodium alginate	/	Extrusion 3D bioprinting of SW480 colorectal cancer cells with macrophages and endothelial cells models the tumor microenvironment for drug screening	48
		Human	HCT116,PDOs	3–5 d	Microextrusion 3D bioprinting	barrel temperature = 25 °C; nozzle inner diameter/ specification = 25 G; extrusion pressure = 0.2 bar; extrusion time = 0.4 s; printing platform temperature = 4 °C	GelMA/adECM	/	Microextrusion 3D bioprinting of patient-derived colorectal cancer organoids in GelMA/ adECM composite bioink enables high-throughput personalized drug screening	37
		Human	PDOs	10 d	Pneumatic extrusion 3D bioprinting	25 gauge (0.25 mm) nozzle; pressure 8–10 kPa; speed 15 ms with 200 ms preflow delay	Alginate with RGD/ nanofibrillar cellulose	/	Pneumatic extrusion 3D bioprinting of patient-derived colorectal cancer metastases enables long-term organoid screening for oncolytic viral-delivered chemotherapy	49
		Human	PDOs	10 d	Embedded bioprinting/Extrusion-based bioprinting	Printing PCL wall: continuous pressure 150 kPa, nozzle diameter 200 μm; bath-ink (alginate bath) extrusion: extrusion rate 0.046 mL/s, nozzle diameter 300 μm	GelTex (50% v/v)/gelatin/HA	1.5% (w/v) alginate-gelatin/ HA	Embedded extrusion bioprinting of patient-derived CRC organoids in stiff alginate enables uniform arrayed models for personalized precision medicine	30
	Carcinoma of the stomach	Human	PDOs	10 d	Photopolymerization-based 3D bioprinting	Structural dimensions and geometry: construction 6 mm × 6 mm × 0.8 mm; layer height 0.2 mm, line width 1.0 mm; printing speed: extrusion speed 1 mm^3/s, printing speed 6 mm^3/s	6.25% GelMA, 0.5% HAMA, 0.125% LAP	/	Photopolymerization-based 3D bioprinting of patient-derived gastric cancer cells predicts chemotherapy responses and enables personalized precision medicine	37

(*Cont'd...*)

Table 1. (*Continued*)

System	Organ	Species	Cell line	Culture time	Method	Printing parameter	Bioinks	Support bath	Summary	Ref
		Human	HGC27	7 d	Photopolymerization-based 3D bioprinting/ Extrusion-based bioprinting	25 G nozzle; moving speed: 360 mm/min; layer height: 0.22 mm; 4 layers (total height: 0.88 mm); model side length: 1.5 cm. Linear filling spacing: 1.5 mm; each layer was rotated 90° and repeated twice. Pneumatic pressure: 25–35 kPa	GelMA + 0.25% (w/v) LAP	/	Photopolymerization-based 3D bioprinting of patient-derived gastric cancer cells enables rapid drug screening and personalized precision medicine prediction	34
	Pancreatic carcinoma	Human	hT1/PANC-1	24 h	Magnetic force-assisted bioprinting	4 h magnetic drive	NanoShuttle-PL	/	Magnetic force-assisted 3D bioprinting of patient-derived pancreatic cancer organoids enables high-throughput phenotypic drug screening for precision medicine	50
		Human	hT1/hM1A	24 h	Magnetic force-assisted 3D bioprinting	4 h magnetic drive	NanoShuttle-PL	/	Magnetic force-assisted 3D bioprinting of patient-derived pancreatic cancer organoids enables large-scale high-throughput drug screening	51
Reproductive system	Breast cancer	Human	MCF-7/ MDA-MB-468	7 d	CNC-controlled micropipette bioprinting	Nozzle/tip: glass-drawn micropipette, tip diameter 50 μm; deposition amount and cell number: 40 cells/ injection event, and each deposition 66 nL/injection event; array spacing: linear array 300 μm, circular array 500 μm; printing temperature: heating printing platform 37 °C	Collagen I	/	Open-source CNC-controlled bioprinting generates mammary tumor organoids and chimeric structures with microenvironmental epigenetic reprogramming	52
		Human	MCF-7/ MDA-MB-468	14 d	CNC-controlled glass micropipette bioprinting	When 3D printing, a CNC-driven toolpath is used to generate the path; the number of cells per injection site: 50 (±3) cells; injection point spacing: 500 μm intervals	huMECM/ GelTrex	/	CNC bioprinting of cells in decellularized mammary ECM hydrogels reveals tissue-specific microenvironmental control of organoid morphogenesis	53

(*Cont'd...*)

doi: 10.36922/IJB026400430

Table 1. (*Continued*)

System	Organ	Species	Cell line	Culture time	Method	Printing parameter	Bioinks	Support bath	Summary	Ref
		Human	21PT/ MDA-MB-231	7 d	Extrusion-based 3D bioprinting	Printing needle: 22G or 27G; printing pressure: 0.4 ± 0.1 bar; printing speed: 22 G is 4 mm/s, 27 G is 7 mm/s; collagen was printed into an SF support bath with a thickness of 5 mm	Collagen–HA–pNIPAM	silk fibroin	Embedded bioprinting of low-concentration collagen-based bioink in silk support bath recapitulates tumor microenvironment heterogeneity	54
		Human	BT-474/MCF-7	3 d	Extrusion-based bioprinting	Incubation before printing: incubation at 17 °C for 30 min; printing pressure: 7–15 kPa in a 96-well plate (and describe cell viability in the range of 10–25 kPa control comparison)-needle: 25 gauge for comparison, inner diameter 260 μm	Mammocult	Matrigel	Bioprinted 3D breast cancer organoids enable high-throughput drug screening and personalized medicine approaches	35
		Human	MCF-7/ MDA-MB-231	7 d	Microinjection-based 3D bioprinting	Needle/nozzle: P-1,000 glass needle, tip about 100 μm (needle volume: 25–50 μL); injection site: about 100 cells per injection site; grid: 3 × 10 layout, 300 μm column spacing, 1.5 mm row spacing	Collagen	/	Microinjection 3D bioprinting reveals mitochondrial transfer mediates cancer-epithelial interactions in collagen matrices	55
Nervous system	Glioma	Human	U118/GBM4	3 w	Kenzan	Needle array: 9 × 9 array; needle diameter: 0.17 mm; needle bed pitch (needle spacing): 0.40 mm; available size: 3.20 mm square × 10.0 mm height; inlet/outlet nozzle: 27-gauge nozzle, inner diameter: 0.19 mm	Noble agar	/	Scaffold-free 3D spheroid co-cultures recapitulate glioma invasion into neural tissue, enabling real-time invasiveness visualization	56
		Human	GBM 1/GBM 2	7 d	Immersion bioprinting	About 20 μL of bioink was deposited in each hole. UV crosslinking: 365 nm, 18 W / cm2, about 1 s/pore; after cross-linking, the plate was briefly transferred to 37°C to reduce the viscosity of gelatin	Coll-MA/ PEGDA	10 mg/mL gelatin	Immersion bioprinting of collagen-HA bioink enables patient-derived tumor organoid culture and high-throughput drug screening	57
		Human	Glioblastoma stem cellss	10 d	Light-based 3D bioprinting	DMD light curing: core 20 s exposure, peripheral 15 s exposure; the cell suspension was mixed with the prepolymer at 1:1 and printed immediately	8% (w/v) GelMA + 0.5% (w/v) GMHA	/	A light-based 3D bioprinted tetra-culture glioblastoma model mimics the tumor microenvironment to improve drug screening accuracy	58

(*Cont'd...*)

Table 1. (*Continued*)

System	Organ	Species	Cell line	Culture time	Method	Printing parameter	Bioinks	Support bath	Summary	Ref
		Human	PDOs	4 d	Automated magnetic 3D bioprinting	Ferromagnetic coating volume: 10 μL; magnetic ink formulation: 1 wt% MNPs in 0.025 wt% CNF; coating time: 30 min; magnetic rod diameter: 2 mm. Electromagnet voltage: 15 V	1 wt% MNPs/0.025 wt% CNF	0.50 wt% CNF	Automated magnetic bioprinting of neural organoids and tumor spheroids enables scalable assembloid fabrication and drug screening	59
		Human	GBM	7 d	Immersion bioprinting	Bioprinter: Cellink BIO X, using syringe pump printhead; spray needle: 22 G × 1/2'blunt tip; generated volume: about 10 μL; extrusion rate: 5μL/s	HA/LAP	Hyaluronic acid support bath	This study demonstrates immersion bioprinting of human cancer organoids for drug-testing applications	57
Urinary system	Bladder	Human	PDOs	7 d	Inkjet printing	The nozzle diameter was 80 μm. The applied voltage was ± 80 V; under the condition of "try to obtain single-cell drops": cell concentration 5×10^5 cells/mL, printing frequency 2 Hz	Matrigel	/	This study utilizes inkjet printing to create human bladder tumor organoids for drug response analysis	60
	Renal carcinoma	Human	RCC	14 d	High-throughput bioprinting	25-gauge needle; printing environment: 15°C incubation temperature, 4°C printing chamber temperature; extrusion speed: 10 mm^3/min; the network hydrogel structure was maintained in 2% $CaCl_2$ for 3 min	30% Matrigel, 3.75% gelatin, 1% sodium alginate	2% $CaCl_2$	This study uses extrusion bioprinting to create patient-derived renal cancer organoids for high-throughput drug screening	38
	Carcinoma of the prostate	Human	PC3	3 d	Aspiration-assisted bioprinting	Sartorius CellCelector: Suction volume 2 μL, suction speed 5%; the size of the capillary is 1/5–1/4 of the spheroidal diameter	PDMS/PEGDA/ GelMA	jammed granular hydrogel	This study explores microfluidic and DLP 3D printing for microgel fabrication and organoid/ spheroid manipulation	61

(*Cont'd...*)

Table 1. (*Continued*)

System	Organ	Species	Cell line	Culture time	Method	Printing parameter	Bioinks	Support bath	Summary	Ref
Respiratory system	Lung cancer	Human	LCOs	2 d	Microextrusion-based 3D bioprinting	PEVA was extruded through a 25 G metal nozzle after melting, and the pneumatic pressure was 500 kPa. UV sterilization for 1 d; lCO printing: the printing pressure in the iLFs region is 5–12 kPa	LudECM/ Matrigel/PEVA	/	This study uses microextrusion bioprinting with decellularized lung matrix to create vascularized human lung cancer organoids	62
Endocrine system	Thyroid cancer	Human	DEOs	10 d	Microfluidic 3D bioprinting	UV sterilization for 30 min before printing; Matrigel was used as the printing material when printing; volume = 100 μL	Matrigel	/	This study uses microfluidic bioprinting to create patient-derived thyroid cancer organoids for drug screening and metastasis modeling	63

Abbreviations: 3D: Three-dimensional; 5-FU: 5-Fluorouracil; adECM: Adipose-derived extracellular matrix; CAFs: Cancer-associated fibroblasts; $CaCl_2$: Calcium chloride; CNC: Computer numerical control; CNF: Cellulose nanofiber; DLP: Digital light processing; DMD: Digital micromirror device; ECM: Extracellular matrix; GBM: Glioblastoma; GelMA: Gelatin methacryloyl; GMHA: Glycidyl methacrylated hyaluronic acid; HA: Hyaluronic acid; HAMA: Hyaluronic acid methacrylate; IIFK: Ile-isoleucine-phenylalanine-lysine; IKVAV: Isoleucine-lysine-valine-alanine-valine; LAP: Lithium phenyl-2,4,6-trimethylbenzoylphosphinate; LCOs: Lung cancer organoids; MNPs: Magnetic nanoparticles; PBS: Phosphate-buffered saline; PDOs: Patient-derived organoids; PDMS: Polydimethylsiloxane; PEGDA: Poly(ethylene glycol) diacrylate; PEVA: Poly(ethylene-co-vinyl acetate); RCC: Renal cell carcinoma; RGD: Arginine-glycine-aspartic acid; SAW: Surface acoustic wave; SF: Silk fibroin; UV: Ultraviolet.

doi: 10.36922/IJB026400430

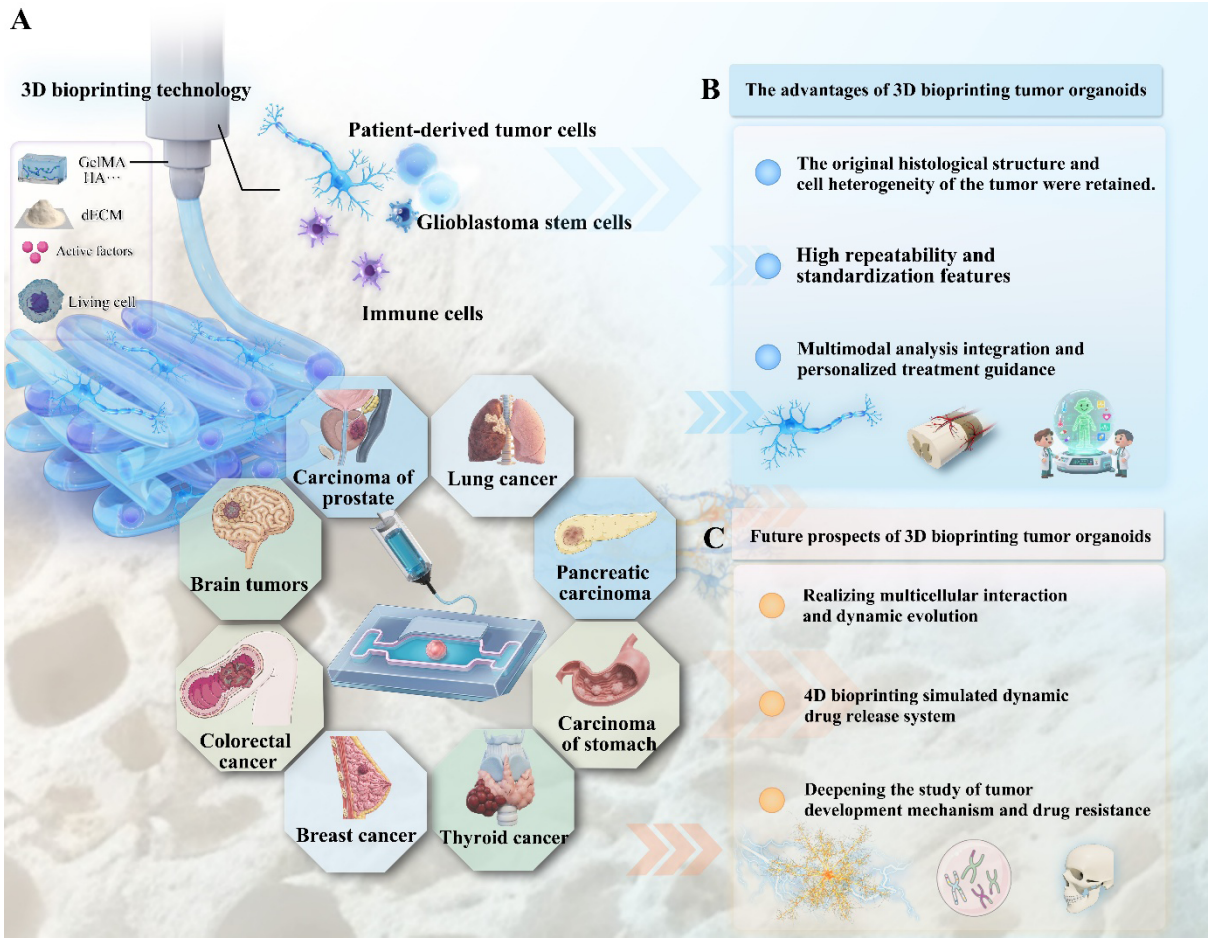


Figure 1. Schematic diagram of 3D bioprinted tumor organoid technology. (A) The printing technology principle. By combining biomaterials such as GelMA/IIA and extracellular matrix with patient tumor cells, stem cells, and immune cells, organoid models of multiple cancer types can be constructed (brain tumors, prostate cancer, lung cancer, pancreatic cancer, colorectal cancer, breast cancer, thyroid cancer, gastric cancer). (B) The three major advantages of this technology are preservation of the tissue structure and cellular heterogeneity of the original tumor, high reproducibility and standardization, and support for multimodal analysis and the development of personalized treatment strategies. (C) Future directions include studying multicellular interactions, developing 4D dynamic drug-release systems, and deepening research on tumor drug-resistance mechanisms, providing an innovative platform for precision medicine and personalized cancer treatment.
Abbreviations: 3D: Three-dimensional; 4D: Four-dimensional; dECM: Decellularized extracellular matrix; GelMA: Gelatin methacryloyl; HA: Hyaluronic acid.

2. Bioprinting techniques

From a translational perspective, no single bioprinting modality can fully satisfy the competing requirements of cell viability, spatial resolution, throughput, and construct complexity. Therefore, the selection of printing strategy should be matched to the biological question: extrusion-based printing is suitable for cell-rich and mechanically stable constructs, inkjet-based printing is advantageous for precise low-volume deposition and high-throughput screening, whereas lithography-based printing offers superior spatial resolution for reproducing fine microarchitectures. In tumor organoid applications, the choice of printing strategy is therefore not simply technical, but directly determines the degree to which tissue architecture, microenvironmental gradients, and multicellular organization can be reconstructed. Understanding these modality-specific strengths and limitations is essential for rational model design and for selecting the most appropriate platform according to the biological question being addressed.

2.1. Extrusion-based bioprinting

Extrusion-based bioprinting is a widely used 3D bioprinting technology, whose core working principle is

to continuously extrude viscous bioink from a fine nozzle or needle through mechanical force (such as piston, pneumatic, or screw-driven), depositing it layer by layer along a preset 3D path to ultimately construct the target structure.[64-67] This printing method places high demands on the rheological properties of the bioink, typically suitable for gel-like materials with a certain viscosity and shear-thinning behavior, such as alginate, gelatin, collagen, gelatin methacryloyl (GelMA), and various synthetic polymer hydrogels.[68-70] These materials must withstand the shear stress during extrusion without damaging encapsulated cells and must rapidly solidify after deposition to maintain structural integrity.[71,72] Its limitations lie in the fact that high-viscosity bioinks may exert mechanical stress on cells, affecting cell viability; meanwhile, printing resolution is limited by the nozzle diameter, making it difficult to achieve micron-level fine structures, which poses a challenge for simulating the complex microvascular networks or the nanostructures of the extracellular matrix *in vivo*.[73-75] However, extrusion-based bioprinting also has unique advantages, such as relatively simple operation, lower cost, the ability to encapsulate high-density cells, printing larger-sized structures, and multi-material compatibility. Particularly in constructing tumor organoid models, extrusion-based bioprinting can effectively simulate the solid tumor characteristics of tumors,[76-78] replicate the physical and biochemical cues of the tumor microenvironment by customizing bioink compositions, and precisely control the spatial distribution of different cell types (such as tumor cells, fibroblasts, immune cells, and vascular endothelial cells), thereby constructing more physiologically relevant tumor organoids, which is crucial for studying tumor heterogeneity, cell-cell interactions, and drug penetration.[79-81]

To overcome the inherent limitations of traditional extrusion-based bioprinting and meet the growing demands of complex tissue engineering, a series of emerging derivative technologies are continuously being developed. These technologies not only improve printing precision and cell viability but also expand the range of printable bioinks. For example, fused deposition modeling bioprinting is primarily used to fabricate thermoplastic scaffolds and is distinct from direct cell-laden bioprinting; because it requires molten polymer processing at elevated temperatures, it is generally unsuitable for direct encapsulation of living cells and is therefore typically combined with subsequent cell seeding or indirect bioprinting strategies.[82-84] Coaxial extrusion technology allows the simultaneous extrusion of two or more bioinks to form fibers with a core-shell structure, which holds great potential for constructing structures with gradient bioactivity or simulating complex conduits such as blood vessels.[85-87] In addition, cryobioprinting uses low-temperature printing together with cryoprotectants to mitigate freezing-induced injury. The printed construct is subsequently stabilized by controlled crosslinking and/or thawing, because freezing–thawing injury may still compromise cell viability.[88-90] In the construction of tumor organoid models, these derivative methods can achieve more refined simulation of the tumor microenvironment, for example by using coaxial extrusion to construct organoids with vascular lumens, or by using composite materials to print matrices with specific mechanical gradients and biochemical signals, thereby more accurately reflecting tumor growth, invasion, and drug response behavior, and providing more reliable *in vitro* models for preclinical studies of personalized treatment strategies[64,91,92] (Figure 2A).

Overall, extrusion-based bioprinting remains the most practical and widely adaptable platform for tumor organoid fabrication because it combines relative simplicity, material flexibility, and multicellular compatibility, making it particularly suitable for constructing structurally robust tumor models and multicellular microenvironment analogs.

2.2. Inkjet-based bioprinting

Inkjet-based bioprinting is a non-contact printing technology whose core principle is similar to that of an office inkjet printer. It uses thermal force (thermal inkjet) or mechanical force (piezoelectric inkjet) to drive liquid bioink and precisely deposit it as tiny droplets onto a substrate, building 3D structures layer by layer.[93-95] Thermal inkjet uses instantaneous heating to generate bubbles that push the ink out, while piezoelectric inkjet generates pressure waves through the deformation of piezoelectric crystals to drive the ink.[96,97] This printing method has relatively low requirements for bioink viscosity and is generally suitable for low-viscosity aqueous solutions or dilute hydrogel precursors, such as diluted alginate, gelatin solutions, collagen solutions, cell suspensions, or growth factor solutions.[98-100] The bioink must be stable enough to avoid nozzle clogging and must solidify or polymerize quickly after deposition.[101,102] Its main limitations are that the cell density that can be encapsulated is usually low, and during printing, thermal inkjet may thermally damage cells, while piezoelectric inkjet may generate shear stress, thereby affecting cell viability.[73,103,104] In addition, the printed structure lacks internal support, making it difficult to construct complex or large-scale macroscopic structures. However, inkjet-based bioprinting also has notable advantages, such as fast printing speed, low cost, non-contact printing that reduces the risk of cross-contamination, high printing resolution that enables

precise deposition of individual cells, and the ability to print multiple materials simultaneous.[105-107] In particular, for bioprinting tumor organoid models, inkjet technology offers unique advantages for constructing highly uniform, controllable, and individualized miniature organoids.[108-110] Its high precision can ensure that each organoid starts with a precise number of cells, and it can simulate the heterogeneity of the tumor microenvironment through fine spatial arrangement, for example, by printing tumor cells, immune cells, and stromal cells in specific ratios and positions, which is of great significance for studying tumor cell-microenvironment interactions, drug screening, and the preclinical development of personalized treatment strategies.[111-113]

To overcome the limitations of traditional inkjet bioprinting in cell viability, printing materials, and structural complexity, and to further enhance its application potential in tumor organoid model construction, researchers are continuously developing a series of emerging derivative technologies.[114,115] For example, inkjet-assisted bioprinting combines the precision of inkjet technology with the structural stability of extrusion technology by precisely depositing cells or bioactive molecules via inkjet and then printing structural scaffolds via extrusion, balancing cell viability and structural complexity.[99,116] Microfluidic inkjet technology integrates microfluidic chips with inkjet printheads, enabling precise control of droplet generation and contents, thus achieving high-throughput, uniform cell encapsulation and organoid formation, and is especially suitable for fine control at the single-cell level.[117,118] Aerosol jet bioprinting is a technology that uses an aerosol airflow to drive droplet jetting, allowing printing with a wider range of material viscosities, including high-viscosity inks and nanoparticles, while also offering higher resolution and smaller droplet sizes, providing the possibility of constructing biological structures with submicron features.[119-121] In constructing tumor organoid models, these derivative approaches can more accurately simulate the microenvironment. For example, using microfluidic inkjet technology, researchers can precisely mix or layer different tumor cell subpopulations, stromal cells, and immune cells for printing to simulate tumor heterogeneity and study interactions between cell types.[122] Aerosol jet bioprinting may be used to construct matrices with nanoscale topological structures to simulate the mechanical and biochemical signals of the extracellular matrix in the tumor microenvironment, thereby more realistically reflecting tumor cell behavior and drug responses. These technologies not only expand the application scope of inkjet bioprinting but also lay the foundation for constructing more complex and functionally more powerful tumor organoid models in the future.[123-125] Therefore, inkjet-based bioprinting is best viewed as a high-precision, high-throughput platform for generating standardized, cell-resolved tumor organoid arrays, especially when the research goal is to control initial cellular composition and spatial patterning rather than build large load-bearing structures.

2.3. Lithography-based bioprinting

Lithography-based bioprinting uses photopolymerization to construct 3D structures.[126,127] Its core working principle is to expose a hydrogel precursor solution (bioink) containing photosensitizers and cells to light of a specific wavelength. The photosensitizer absorbs the light energy and generates reactive free radicals, which initiate crosslinking polymerization of the hydrogel precursor, thereby forming a solid hydrogel structure in the illuminated area.[128-130] By precisely controlling the pattern and depth of illumination (for example, using a digital micromirror device or a photomask), the liquid bioink can be solidified layer by layer, and the uncured portions can be removed, ultimately forming complex 3D structures.[131,132] The bioinks compatible with this printing method are mainly photocrosslinkable hydrogels, such as GelMA, polyethylene glycol diacrylate, and other photoreactive polymers.[128,133] These materials are generally biocompatible, and the curing process is relatively mild. Its main limitations are that light exposure may cause a certain degree of phototoxicity or thermal damage to encapsulated cells, especially under prolonged or high-intensity exposure[134,135], the bioink needs to have good photocrosslinking properties and suitable viscosity to ensure printing accuracy and structural stability; at the same time, material selection is relatively limited, and not all biomaterials are easy to modify for photosensitivity. However, lithography-based bioprinting also offers unique advantages, such as extremely high printing resolution (reaching micron or even submicron levels), the ability to rapidly construct complex, fine structures, and the ability to achieve precise co-culture of multiple materials and multiple cell types.[135-137] In constructing tumor organoid models, this high-precision characteristic of lithography-based bioprinting is particularly critical. It can precisely simulate the microstructure and cell distribution of tumors *in vivo*, for example, by constructing extracellular matrices with specific geometric shapes, porosity, and mechanical gradients, and can even simulate vascular networks or lymphatic structures within tumors.[138,139] This capability offers unique advantages for in-depth study of tumor cell interactions with the microenvironment, tumor invasion and metastasis pathways, and drug diffusion and penetration within tumors.[140-142]

To overcome the limitations of traditional lithography-based bioprinting and further expand its application

scope, a variety of emerging derivative technologies are developing rapidly. For example, stereolithography bioprinting uses a laser to scan point by point across the surface of a liquid photosensitive resin to cure it, achieving high-precision printing, but its layer thickness limits cell viability.[143,144] Digital light processing bioprinting, by contrast, uses a digital micromirror device to project an entire-layer pattern, enabling rapid regional curing that improves printing speed and efficiency while maintaining high resolution, with strong potential for constructing high-throughput organoid arrays.[145,146] Two-photon polymerization bioprinting exploits nonlinear optical effects so that polymerization occurs only at the laser focal point, enabling ultra-high-resolution printing at the nanometer scale and even allowing the construction of subcellular-level structures, providing the possibility of simulating nanoscale physical barriers or signal molecule distributions in the tumor cell microenvironment.[147-149] In addition, live-cell photopatterning technology allows precise control of cell capture and arrangement during light exposure, forming cell patterns at predetermined positions, which is highly significant for studying tumor-cell behavior in specific microenvironments.[150-152] In constructing tumor organoid models, digital light processing bioprinting is widely used to rapidly manufacture 3D organoids with precise morphology and cellular composition, balancing high throughput and high resolution and accelerating drug screening and preclinical evaluation of personalized treatment strategies. Meanwhile, two-photon polymerization provides the possibility of constructing microenvironments closer to physiological conditions, such as simulating the extracellular matrix fiber network of tumor tissue, enabling researchers to more deeply investigate the influence of microstructures on tumor behavior. These advanced lithography-derived technologies are driving tumor organoid models toward greater realism, greater complexity, and stronger functionality[153-155] (Figure 2B). In this context, lithography-based bioprinting is particularly valuable for applications requiring fine architectural control, such as reproducing extracellular matrix microfeatures, vascular-like networks, and spatially defined tumor niches that are difficult to achieve with conventional printing strategies.

2.4. Bioprinting techniques and bioink-mediated biological control

While the precise deposition capabilities of bioprinting techniques are crucial for establishing the initial geometric architecture of tumor models, the bioink formulations themselves play an equally, if not more, critical role in governing the subsequent biological behavior and functional relevance of the engineered constructs. Bioinks are not merely structural scaffolds; they serve as a dynamic extracellular matrix that dictates cellular responses, including proliferation, invasion, and drug sensitivity. The intricate interplay between the inherent properties of bioinks, such as matrix stiffness, crosslinking conditions, degradation kinetics, and biochemical composition, and cellular biology is paramount for accurately mimicking the complex tumor microenvironment.

For instance, bioink stiffness directly influences tumor cell mechanotransduction pathways, affecting cellular morphology, proliferation rates, and metastatic potential. Crosslinking conditions not only determine the final mechanical properties but also regulate pore size and nutrient diffusion, thereby impacting cell viability and the formation of nutrient/oxygen gradients. The degradation behavior of the bioink is vital for facilitating cell migration, remodeling, and the release of encapsulated therapeutic agents or signaling molecules, closely mirroring the dynamic nature of the *in vivo* extracellular matrix. Furthermore, the biochemical composition, including cell-adhesive motifs, growth factors, or proteolytic cleavage sites, provides specific cues that modulate cell–cell and cell–matrix interactions, thereby influencing tumor spheroid formation, angiogenesis, and immune cell infiltration within the bioprinted model. Therefore, a judicious selection and rational design of bioinks, tailored to specific tumor types and research questions, are indispensable for developing physiologically relevant and predictive 3D tumor models (Table 2).

3. Three-dimensional bioprinted tumor organoids

3.1. Digestive system

3.1.1. Colorectal cancer

Three-dimensional bioprinting technology for early-stage colorectal cancer tumor organoid construction mainly focuses on screening and optimizing bioink materials. By combining colorectal cancer cell lines with different bioinks through extrusion-based 3D bioprinting, the feasibility of traditional materials such as alginate and gelatin was systematically evaluated, proving they can maintain 90% cell viability after printing[46] (Figure 3A). Subsequently, to meet high-throughput application needs, researchers developed composite bioink systems with photo-crosslinking properties, increasing the survival rate of tumor organoids after printing to 97%, while maintaining the multicellular polarity structure consistent with traditional Matrigel culture[29] (Figure 3C). This series of material innovations laid the foundation for constructing more complex tumor micro-tissues.

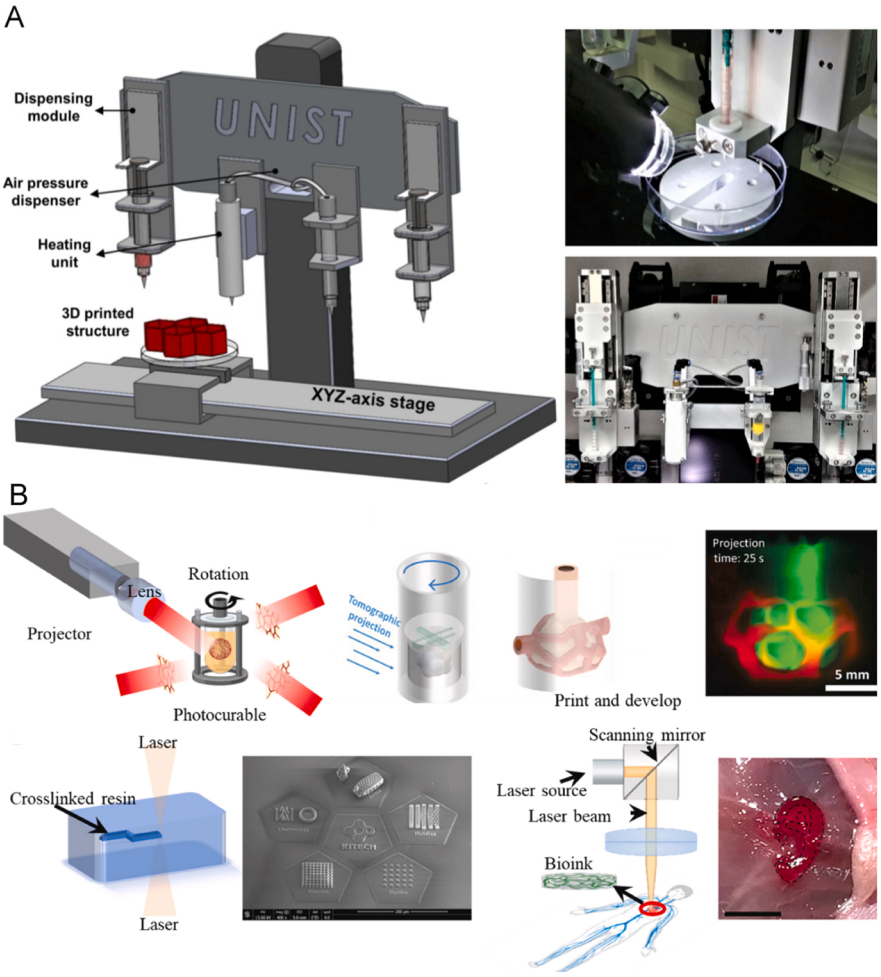


Figure 2. Implementation of three-dimensional bioprinting technology. (A) A three-dimensional bioprinting setup is shown, including a three-axis motion platform and a jetting device. The photograph shows a jetting module with four printing nozzles, as well as a three-dimensional printing operation using decellularized extracellular matrix bioink. Reprinted from Cui *et al.*[156] (B) The working principle of light-induced bioprinting is schematically illustrated. Reprinted from Liu *et al.*[157]

As printing technology has improved, 3D bioprinting has evolved from simple single-cell organoid printing to the construction of patient-derived multicellular systems. The application of acoustic bioprinting technology enables researchers to precisely encapsulate patient-derived cancer-associated fibroblasts and tumor organoids to construct 3D cancer invasion models, achieving real-time monitoring of patient-specific cancer cell migration and invasion kinetics.[47] Furthermore, by integrating multiple cell types (such as tumor cells, tumor-associated macrophages, and endothelial cells) into the printing system, the constructed 3D multicellular models exhibit significantly enhanced tumor-associated gene expression, with IC_{50} values closer to *in vivo* physiological states.[48] This marks a shift in 3D bioprinting from constructing simple tissues to reconstructing the patient-specific tumor microenvironment.

The ultimate application value of 3D bioprinting technology in colorectal cancer research lies in its potential to evaluate preclinical drug responses and inform the development of personalized treatment strategies. However, direct clinical decision-making based solely on these models requires robust prospective validation with large patient cohorts. By evaluating acoustic bioprinting and alignment of patient-derived tumor organoids, a point-to-point detection system capable of modeling cancer invasion and predicting 5-fluorouracil chemotherapy response was established, creating a quantitative correlation between the organoid invasion speed and the patient's clinical spread speed, which could provide an objective basis for further clinical investigation regarding.[19] This

Table 2. Impact of bioink properties on tumor model biological behavior

Bioink type (Example)	GelMA (Gelatin methacryloyl)	Alginate	Collagen (Type I/IV)	Hyaluronic acid (HA)	Decellularized extracellular matrix (dECM)
Key biochemical composition	Modified gelatin (collagen-derived), RGD motifs, MMP cleavage sites	Polysaccharide (guluronic/mannuronic acid), inert	Major ECM protein, RGD, MMP cleavage sites	Glycosaminoglycan, CD44/RHAMM binding sites	Complex mix of native ECM proteins (collagen, elastin, proteoglycans, GAGs) and growth factors
Typical matrix stiffness range	Tunable (kPa to MPa), often softer for cells (0.5–20 kPa)	Broadly tunable (kPa to >100 kPa), often stiffer for structural integrity	Soft (hundreds Pa to few kPa), strain-stiffening behavior	Soft (tens Pa to kPa), often chemically modified for crosslinking	Highly variable, often very soft to stiff (kPa to MPa), tissue-specific
Crosslinking conditions (key aspects)	Photo-polymerization (UV/Vis light, photoinitiators); user-defined intensity/time	Ionic crosslinking (e.g., Ca^{2+}); rapid, reversible, pH-sensitive	pH/temperature-induced self-assembly; enzymatic (transglutaminase)	Chemical (e.g., thiolated HA + PEGDA), enzymatic (transglutaminase), photo-polymerization	Physical (thermal gelation), chemical (e.g., EDC/NHS), enzymatic, photo-crosslinking
Degradation behavior (key aspects)	Enzyme-mediated (MMP-responsive), tunable rate by GelMA concentration/crosslinking density	Very slow/non-degradable in mammalian systems (unless modified or dissolved)	Enzyme-mediated (MMP-responsive), degradation rate depends on density	Enzyme-mediated (hyaluronidase), tunable via modification/crosslinking	Enzyme-mediated (MMP-responsive), highly variable based on source tissue/decellularization
Impact on tumor cell proliferation	Promotes due to RGD; can be restricted by high stiffness/density	Limited by lack of specific cell-binding sites; often requires RGD modification	Supports proliferation; stiffness-dependent (e.g., softer for ductal, stiffer for invasive)	Supports proliferation, especially in early stages; often combined with other bioinks	Highly promoted due to native growth factors/cues; tissue-specific effects
Impact on tumor cell invasion	Facilitated by MMP-mediated degradation; restricted by high crosslinking	Generally restricted due to lack of degradation and cell adhesion	Promotes through matrix remodeling/degradation; stiffness-dependent	Can facilitate or restrict depending on modification/stiffness; CD44 interaction	Strongly promotes due to native structural integrity and cues; cell-specific
Impact on drug penetration	Can be hindered by dense crosslinking; pore size dependent	Primarily diffusion-limited by pore size; non-degradable nature	Influenced by fiber density and alignment; good for macromolecule penetration	Influenced by hydrogel density and charge; can serve as a diffusion barrier	Mimics *in vivo* diffusion behavior; dependent on tissue source/density
Impact on cellular interactions	Supports cell–cell and cell–ECM adhesion; can be co-printed with other cells	Poor inherent cell adhesion; often mixed with other biomaterials for cell integration	Highly supportive of cell adhesion, migration, and signaling	Modulates cell-cell/cell-ECM interactions via CD44; anti-adhesive at high concentrations	Supports diverse cell–cell/cell–matrix interactions, immune modulation
Advantages for TME mimicry	Bioactive, tunable stiffness/degradation, good printability, cell-friendly	Biocompatible, cost-effective, rapid gelation, good mechanical stability	Native ECM component, highly bioactive, excellent cell compatibility	Bioactive, supports cell migration/proliferation, anti-inflammatory, tunable	Most biomimetic, comprehensive native cues, tissue-specific properties
Challenges/limitations	Potential photo-toxicity, swelling, batch variability of gelatin	Lacks bioactivity, slow degradation, requires surface modification for cell adhesion	Mechanically weak, rapid degradation, poor printability (low viscosity), batch variability	Rapid degradation (native HA), poor inherent printability (low viscosity), modification required	Complex preparation, batch variability, mechanical inconsistency, variable printability

Abbreviations: 3D: Three-dimensional; CD44: Cluster of differentiation 44; dECM: Decellularized extracellular matrix; EDC: 1-Ethyl-3-(3-dimethylaminopropyl)carbodiimide; ECM: Extracellular matrix; GelMA: Gelatin methacryloyl; GAGs: Glycosaminoglycans; MMP: Matrix metalloproteinase; NHS: N-Hydroxysuccinimide; PEGDA: Poly(ethylene glycol) diacrylate; RGD: Arginine-glycine-aspartic acid; RHAMM: Receptor for hyaluronan-mediated motility; TME: Tumor microenvironment; UV: Ultraviolet.

doi: 10.36922/IJB026400430

correlation is retrospective, and prospective studies are needed to establish its predictive performance for clinical outcomes. Furthermore, patient-derived organoid arrays constructed via embedded bioprinting can accurately reproduce the tumor microenvironment characteristics of colorectal cancer (including matrix stiffness and hypoxic conditions) and have enabled the development of a label-free prediction model based on supervised learning through morphological features[30] (Figure 3B). At the same time, this technology has also been validated for long-term screening of oncolytic viruses delivering chemotherapy drugs, as printed organ models established from patient metastases maintained stability for several months, which is expected to significantly reduce the need for animal experiments.[49] These advancements indicate that 3D bioprinting has evolved from the technical validation stage to a sophisticated preclinical platform for precision medicine research, offering valuable insights that may inform future clinical decision-making. However, direct clinical applicability as a decision-making tool requires extensive prospective validation studies. Collectively, recent colorectal cancer studies suggest that bioprinting has evolved from a material optimization tool into a platform capable of integrating tumor cells, stromal cells, and functional readouts for individualized drug-response evaluation. The most notable progress has been the shift toward patient-derived multicellular arrays and label-free quantitative evaluation, which together improve the translational relevance of colorectal tumor organoid models.

3.1.2. Gastric cancer

Three-dimensional bioprinting technology for gastric cancer models has overcome the limitations of traditional *in vitro* models by using biomaterials to better simulate the complexity of the tumor microenvironment. GelMA hydrogel, a biomimetic extracellular matrix-like material, was first used in 3D bioprinting gastric cancer models, where its adjustable mechanical properties enable precise control of cell behavior. This GelMA-based 3D printing model not only accurately simulates key malignant characteristics of gastric cancer, such as cell proliferation, invasion, migration, angiogenesis, and the Warburg effect, but also demonstrates high consistency with patient-derived xenograft models in terms of gene expression and drug response, reporting the key role of GelMA in gastric cancer research for the first time[34] (Figure 4C and 4D).

Compared with patient-derived organoids and xenograft models, which are costly and prone to batch effects, 3D bioprinting technology has successfully constructed individualized 3D bioprinted gastric cancer models for 33 gastric cancer patients by optimizing the mechanical properties and biocompatibility of bioinks. These models retain the characteristics of primary tumors in histopathological architecture, biomarker expression abundance, and genetic mutation profiles, while drug-sensitivity screening results show a significant correlation with clinical efficacy in patients, suggesting potential for personalized selection of neoadjuvant and adjuvant chemotherapy drugs. This correlation, however, represents a retrospective analysis, and further prospective clinical studies with robust validation designs and specified predictive performance metrics are necessary to confirm its clinical utility[37] (Figure 4A and 4B). This marks the transformation of 3D bioprinting from a cost-effective technological innovation into a promising platform for precision oncology research, potentially informing future clinical decision-making. However, moving toward direct clinical decision support requires rigorous prospective clinical validation. These studies indicate that gastric cancer bioprinting has progressed from reproducing tumor morphology toward preserving patient-specific histopathological, genomic, and pharmacological features. Among recent advances, using individualized bioprinted gastric cancer models to predict clinical chemotherapy responses represents a particularly important step toward practical precision oncology.

3.1.3. Pancreatic carcinoma

A key breakthrough in 3D bioprinting technology for pancreatic cancer drug screening is addressing heterogeneity and the high costs of traditional 3D organoid culture methods. By combining cell-repellent surfaces with magnetic bioprinting technology, researchers have consistently produced homogenized organoids in standard 384-well and 1,536-well flat-bottom plates, enabling high-throughput screening. This technology has been validated for compatibility with high-throughput screening automation workflows, demonstrating its effectiveness in evaluating drug sensitivity in *KRAS*-mutant patient-derived primary pancreatic cancer cells, including cancer-associated fibroblasts, through a pilot cytotoxicity screen of approximately 3,300 approved drugs.[50] This technological innovation has turned large-scale, standardized high-throughput screening based on an individual patient's tumor from theory into reality.

Building on this technological foundation, researchers achieved the largest 3D model drug screen for pancreatic cancer to date—a high-throughput screening of over 150,000 molecules. This work demonstrated, for the first time, the feasibility of screening at this scale using clinically relevant 3D pancreatic tumor models derived directly from patient biopsies. During the screening process, four unique compound series were identified, exhibiting

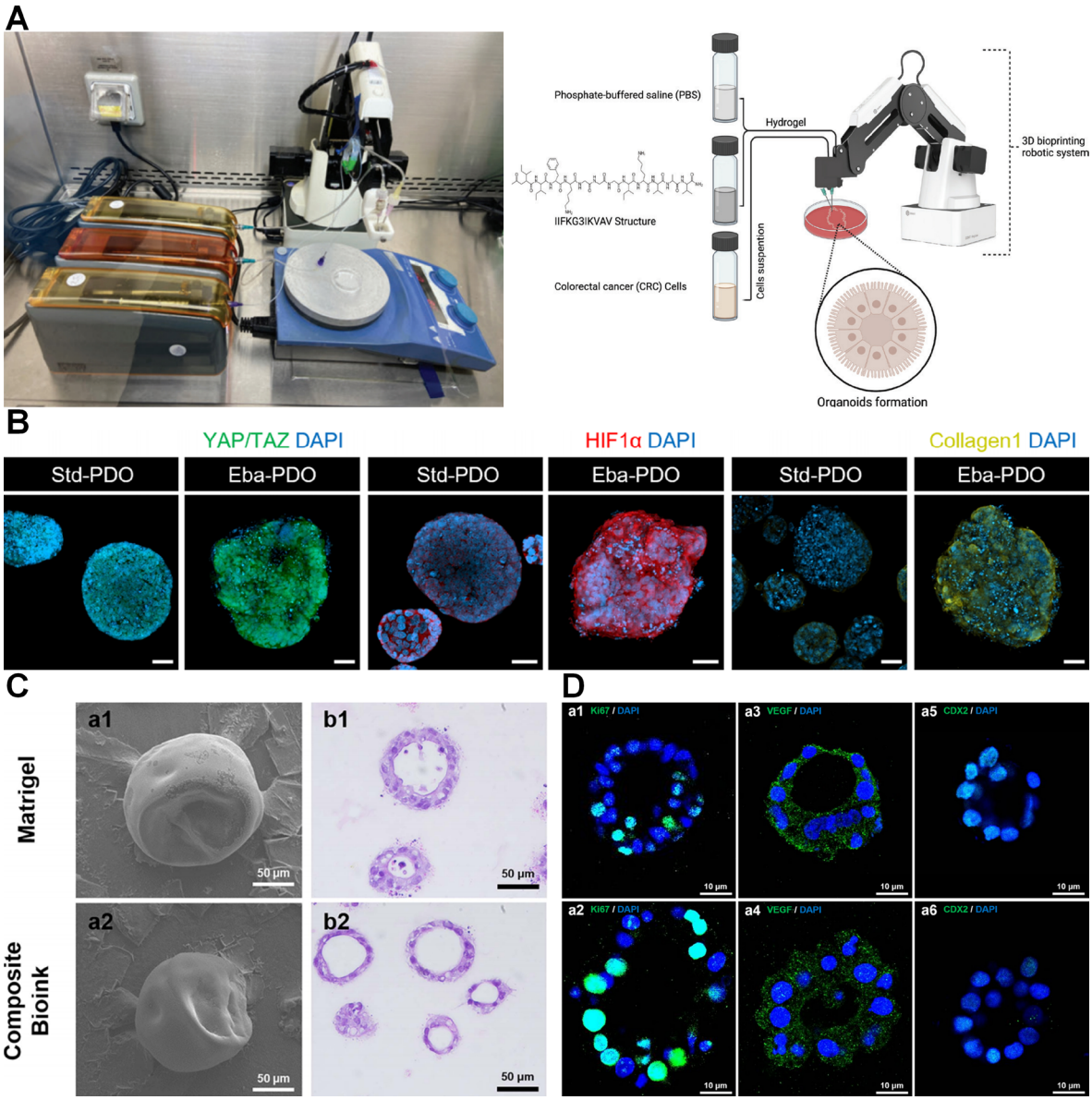


Figure 3. 3D bioprinted colorectal cancer organoid model. (A) Three-dimensional-printed construct using IIFK: IDP hydrogel. In-house bioprinting setup with a robotic arm. Reprinted from Pérez-Pedroza *et al.*[32] (B) Immunofluorescence microscopy images representing the tumor pathophysiological environment, including YAP/TAZ (indicating mechanical stress), HIF1α (indicating hypoxia), and type I collagen (indicating extracellular matrix remodeling). Immunofluorescence microscopy images labeled with YAP/TAZ. Reprinted from Han *et al.*[30] (C) Spatial morphology of three-dimensional bioprinted colorectal cancer organoids. (a1), (a2) scanning electron microscopy and (b1), (b2) H&E staining images show the spatial morphology of colorectal cancer tissue cultured in different hydrogel materials for 7 d. Scale bar: 50 μm. (D) Protein levels of 3D bioprinted colorectal cancer organoids. (a) Immunofluorescence staining of (a1), (a2) Ki67, (a3), (a4) VEGF, and (a5), (a6) CDX2 in the colorectal cancer organoids cultured in the Matrigel and the composite bioink for 5 d. Reprinted with permission from Dai *et al.*[29] Copyright © 2024, IOP Publishing Ltd. Compared with traditional Matrigel, the composite bioink can not only support normal growth and proliferation of colorectal cancer organoids but also maintain the expression levels of proteins related to the pathophysiological characteristics of tumor tissues.

sub-micromolar or even low-nanomolar potency. More importantly, by validating the potency of lead compounds in autologous cancer-associated fibroblasts, researchers found that their selectivity for cancer cells was higher than that for wild-type primary cells, a discovery that laid the foundation for subsequent clinical translation.[51] These initial lead compounds have been validated with consistent results across multiple independent research institutions,

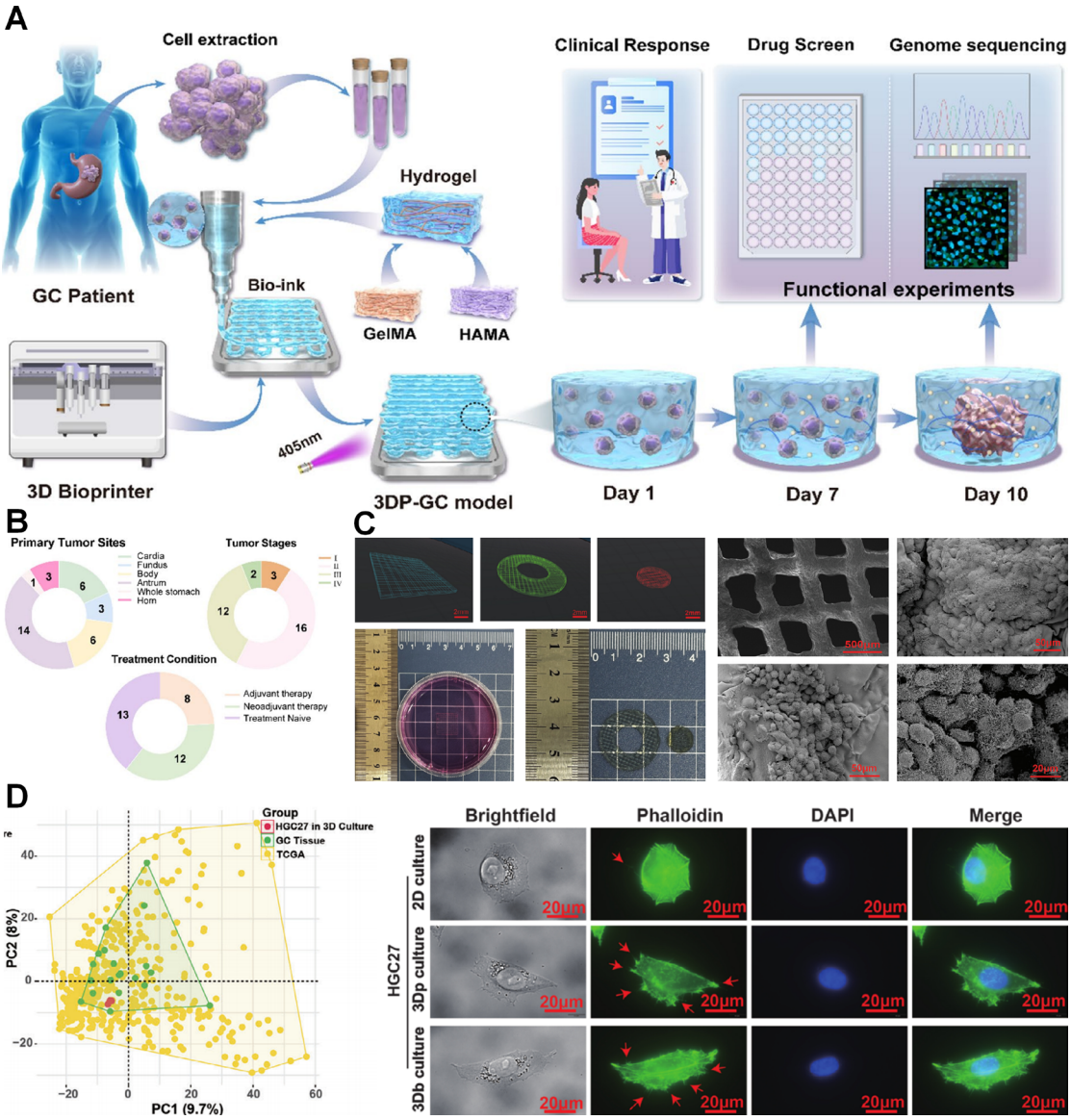


Figure 4. 3D bioprinted gastric cancer organoid model. (A) Schematic diagram of the fabrication process of patient-derived 3DP-GC models and their application in predicting patients' clinical drug responses. (B) TNM staging, primary tumor location, and treatment status of patients from whom 33 GC organoids were successfully established. Reprinted from Du *et al.*[37] (C) Computer-aided design (CAD) of a 3D gastric cancer model showing tumor geometry, along with scanning electron microscopy (SEM) images revealing the cellular architecture of tumor spheroids. Scale bar: 500 μm. (D) Principal component analysis of global transcriptomic profiles of GCCs grown in 2D and 3D systems compared with primary GC tissues (left). Cells cultured in 3D were more elongated and exhibited more pseudopodia (indicated by arrows) (right). It was found that the 3Db model could better maintain the proliferation activity of HGC27 cells and make their behavior closer to the physiological state *in vivo*, thus emphasizing the advantages of 3Db model in gastric cancer research. In addition, cells in the 3D model may be more resistant to drugs, which more closely reflects the clinically observed response of tumor cells to chemotherapeutic drugs. Scale bar: 20 μm. Reprinted with permission from Ju *et al.*[34] Copyright © 2025 Wiley-VCH GmbH.
Abbreviations: 3DP-GC: 3D-printed gastric cancer; GC: Gastric cancer; GCCs: Gastric cancer cells; TNM: Tumor, node, metastasis.

marking a turning point for 3D bioprinting technology as it evolves from a technical platform to actually generating new clinically relevant drug leads. In pancreatic cancer, the major advance has been the ability of bioprinting-assisted systems to standardize organoid production and enable large-scale drug screening in a disease known for marked stromal complexity and therapeutic resistance. This transition from heterogeneous organoid generation to reproducible screening platforms is especially important for translating pancreatic organoid research into drug

discovery and patient stratification.

3.2. Reproductive system

An important development direction for 3D bioprinting in constructing breast cancer tumoroid models is optimizing bioinks and matrix materials to more realistically replicate the *in vivo* tumor microenvironment. By developing extracellular matrix hydrogels derived entirely from decellularized rat or human mammary tissues as novel culture substrates, and combining them with 3D bioprinting platforms, the growth of mammary organoids and tumoroids in tissue-specific matrices has been successfully achieved. This approach not only maintains the unique structural and signaling properties of the extracellular matrix, but also triggers differentiated responses from normal mammary cells and breast cancer cells[53] (Figure 5C). Furthermore, because collagen is abundant in solid tumor extracellular matrix but difficult to print due to its low viscosity, researchers optimized bioinks based on low-concentration collagen I combined with thermo-responsive hyaluronic acid-based polymers. Under embedded bioprinting technology, they successfully constructed breast tumoroid models simulating *in vivo* tumor morphology, and even achieved the construction of vascularized tumor models, providing a more realistic platform for deep understanding of tumor cell biology and drug discovery.[54]

Through continuous technical iteration, bioprinting has expanded to study complex interactions between tumors and their microenvironment, as well as enable high-throughput drug screening. With low-cost bioprinting platforms, researchers can precisely generate tumoroid arrays and co-print them with normal mammary epithelial cells to form chimeric organoids, simulating and studying the inhibitory effects of the mammary microenvironment on tumorigenesis and the mechanisms that redirect cancer cell fate. For example, some studies for the first time used 3D bioprinting-assisted organoid systems to reveal the key role of intercellular mitochondrial transfer from normal mammary epithelial cells to breast cancer cells in regulating cancer cell proliferation potential[52,55] (Figure 5B). In terms of drug screening, combining bioprinting technology with high-speed live-cell interferometry imaging, researchers developed a high-throughput drug screening workflow capable of quantifying mass changes in thousands of organoids in a label-free and time-resolved manner at single-organoid resolution, thereby identifying organoids that are transiently or persistently sensitive or resistant to specific therapies, offering preclinical insights for the development of personalized treatment strategies[35] (Figure 5A). These advances collectively shift 3D bioprinting in breast cancer research from constructing static models to dynamically analyzing intercellular interactions and drug responses. Recent breast cancer studies underscore the value of bioprinting in reconstructing tissue-specific extracellular matrix contexts and in capturing dynamic tumor–stromal interactions. The emerging integration of bioprinting with single-organoid analysis further suggests that future breast cancer models may support not only drug testing but also mechanistic studies of tumor cell plasticity and microenvironment-driven phenotypic changes.

3.3. Nervous system

3.3.1. Glioblastoma

In glioma model construction, efforts focus on overcoming the limitations of traditional two-dimensional culture and animal models by accurately reproducing the complex tumor microenvironment. Researchers developed rapid 3D bioprinting methods to construct clinically relevant biomimetic tissue models by integrating glioblastoma stem cells with astrocytes, neural progenitor cells, and key immune cells—macrophages into hyaluronic acid-rich hydrogels, successfully simulating patient-derived transcriptomic characteristics and revealing the stemness maintenance, invasion, and drug resistance of glioblastoma stem cells[58] (Figure 6B and 6C). This multicellular, species-matched neural environment model provides a scalable, physiologically relevant platform for exploring drug sensitivity, cell–cell crosstalk, invasion mechanisms, and context-specific functional dependencies, and even immune interactions. Meanwhile, 3D bioprinting also combines with scaffold-free 3D culture technology to construct models of glioma cell invasion into nerve-like tissues, tracking the invasion process of glioma cells through real-time and fixed sample tracking, providing a new tool for understanding glioma invasiveness[56] (Figure 6A and 6D).

To further improve the precision and applicability of glioma organoid models, 3D bioprinting research focuses on precise spatial control and the construction of high-throughput screening platforms. Addressing the issue that traditional organoids are susceptible to plastic deformation, researchers developed the spatially patterned organoid transfer platform, using iron oxide nanoparticle-loaded hydrogels and magnetized 3D printers to achieve precise lifting, transportation, and deposition of organoids, thereby constructing precision assemblies composed of human pluripotent stem cell-derived neural organoids and patient-derived glioma organoids, helping to simulate developmental processes and disease etiology.[59] In addition, to address the challenge of preparing uniform organoids in batches in multi-well plates for high-throughput drug screening, researchers innovatively proposed immersion

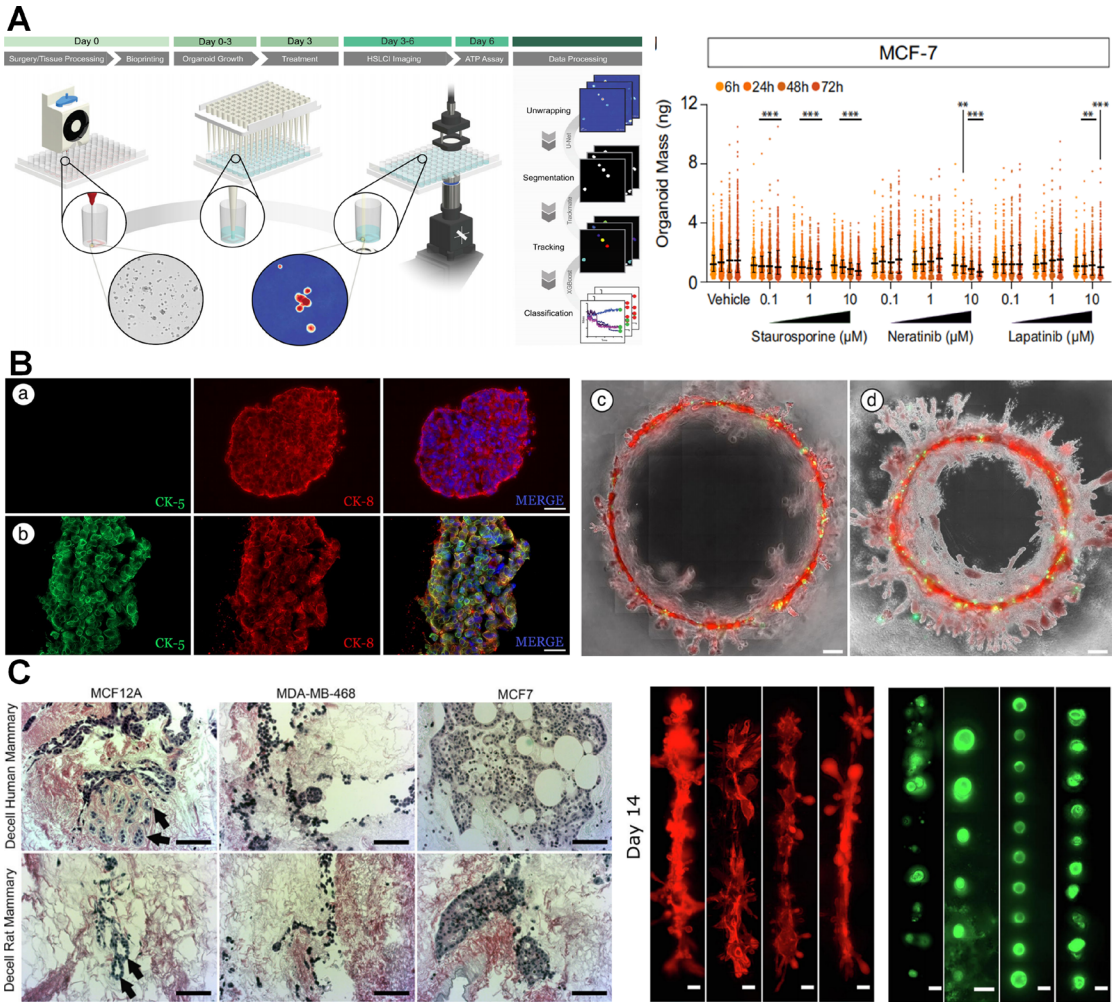


Figure 5. 3D bioprinted breast cancer organoid model. A. Bioprinting enables single-organoid tracking with high-speed live cell interferometry (left). Each line represents the mass distribution at 6, 24, 48, and 72 hours after treatment (right). Reprinted from Tebon *et al.*[35] (B) The bioprinted tumoroids maintained the expected cytokeratin expression and a high proportion of proliferating cells. (a,b) MCF-7 tumors were CK-5 negative (green) and CK-8 positive (red). b) MDA-MB-468 tumor cells were positive for both CK-5 (green) and CK-8 (red). On day 21 (d), a typical large chimeric organoid was produced by 500-micron interval printing of a 5:1 ratio circular print pattern of MCF-12A (red) and MDA-MB-468 (green) cells. Reprinted from Reid *et al.*[52] (C) In decellularized/delipidized mammary tissue, different mammary cell lines exhibited distinct histological behaviors: MCF-12A cells followed the existing luminal structures for orderly arrangement, while MCF-7 and MDA-MB-468 cancer cells grew in a disorganized manner. (D) Using a CNC-controlled microinjection bioprinting platform, MCF-12A (normal mammary epithelium), MCF-7, and MDA-MB-468 (breast cancer cells) were precisely printed (50±3 cells per linear arrangement, 500 μm spacing) in various biological matrices, including GelTrex, rtCOL, rtMECM, and huMECM, for 14-day three-dimensional culture. Reprinted with permission from Mollica *et al.*[53] Copyright © 2019, Wiley-VCH GmbH. It is shown that the bioprinted breast cancer organoids can faithfully maintain the genotypic and phenotypic characteristics of cells. At the same time, it is shown that 3D bioprinting technology has significant advantages in constructing physiologically relevant breast cancer organoids and microenvironment models compared with traditional methods.

Abbreviations: CK-5: Cytokeratin 5; CK-8: Cytokeratin 8; CNC: Computer numerical control; huMECM: Human mammary extracellular matrix; rtCOL: Rat-tail collagen; rtMECM: Rat mammary extracellular matrix.

bioprinting technology. This technology prints bioink composed of hyaluronic acid and collagen into a viscous gelatin bath, effectively preventing interaction between the bioink and pore walls, ensuring spherical morphology and uniformity of organoids, and has been successfully applied to drug screening of patient-derived glioblastoma samples, greatly improving the throughput and efficiency of 3D drug screening.[41] These advances collectively support the use of glioma organoid models as tools for basic research, preclinical personalized drug screening, and research that may facilitate future clinical translation. Overall, glioblastoma bioprinting has advanced from

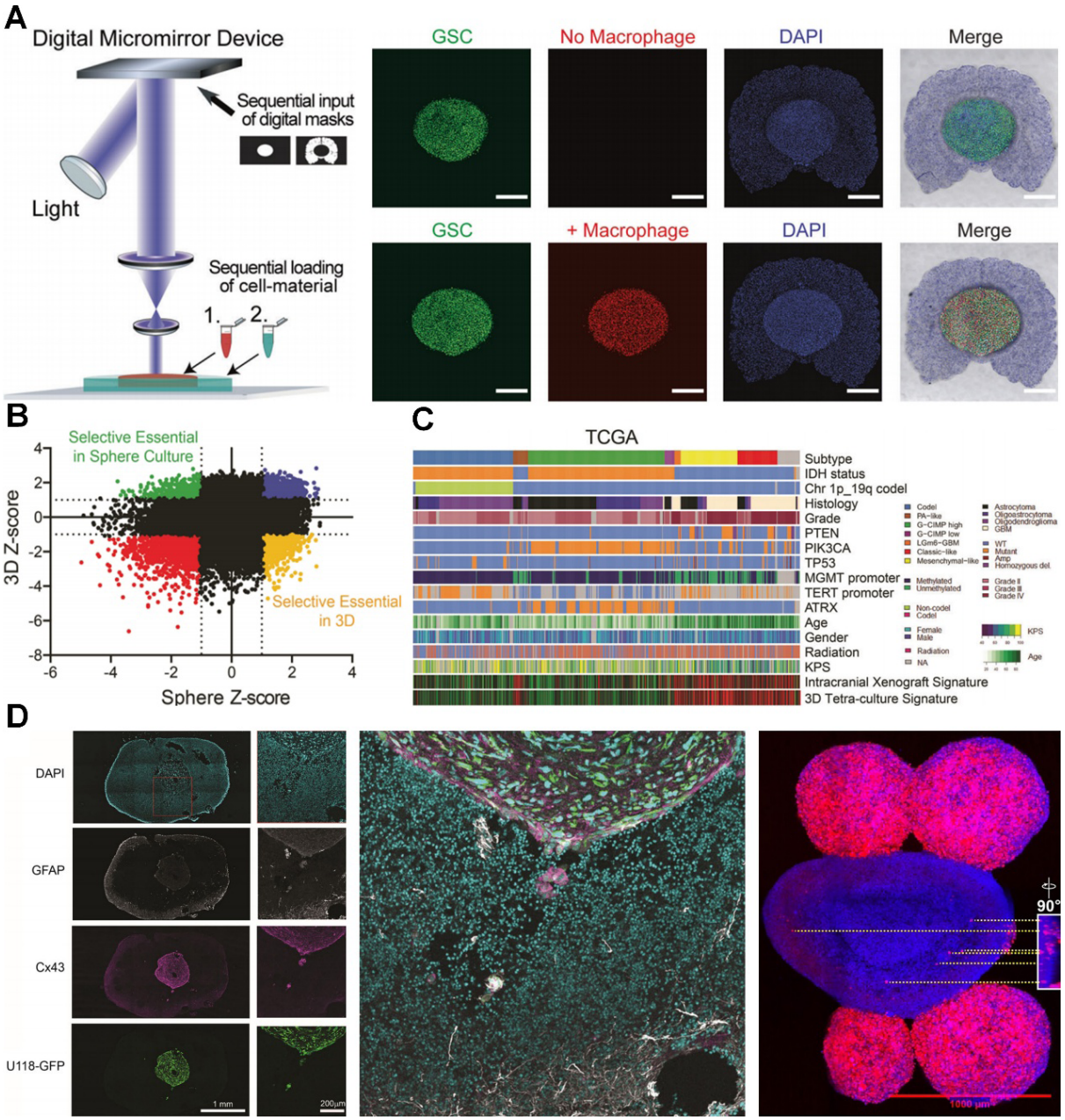


Figure 6. 3D bioprinted glioma organoid model. A. Schematic of a DMD chip-based 3D bioprinting system for creating 3D glioblastoma models (left). Brightfield and immunofluorescence images of the 3D glioblastoma model. GSCs are labeled with green fluorescent protein (GFP), while macrophages are labeled with mCherry (right). Reprinted with permission from Tang *et al.*[58] Copyright © 2020, Center for Excellence in Molecular Cell Science, CAS. (B). Comparison of functionally dependent Z-scores between sphere culture and 3D culture in a four-cell culture model. (C) Heatmap displaying mRNA expression signatures of intracranial xenografts (vs. sphere cell culture) and 3D bioprinted tetra-cultures (vs. sphere cell culture) as defined by the TCGA glioma HG-U133A microarray. Various clinical metrics, patient information, and information on tumor genetics are also displayed. Reprinted with permission from Tang *et al.*[58] Copyright © 2020, Center for Excellence in Molecular Cell Science, CAS. (D) Confocal images showing a section of a cell mass stained for DNA (DAPI), glial cells (GFAP), Cx43, and GFP-labeled U118 cells. The red box in the figure is shown at higher magnification, indicating U118 cells invading the neurosphere (left). Maximum projection of spheroid aggregates. CD1 cells are stained blue, and GBM4 cells are stained red and blue. GBM4 cells can be seen invading the CD1 spheroid (right). Immunofluorescence confocal microscopy successfully visualized the invasion process of U118 glioma cells in bioprinted human neurospheres, while Figure D visually demonstrated the ability of GBM4 glioma cells to invade mouse neural progenitor cell spheres under scaffold-free 3D culture conditions (invasion distance is about 100–200 μm in the xy direction and about 5–30 μm in the z direction), verifying the effectiveness of 3D bioprinting and scaffold-free 3D culture methods in establishing a reliable glioma invasion model. Reprinted with permission from van Pel *et al.*[56] Copyright © 2018, The International CCN Society.

simple invasion modeling to more biologically complete systems that incorporate neural, stromal, and immune components. This is particularly important because glioblastoma progression is strongly shaped by context-dependent cell–cell interactions that cannot be adequately captured in conventional monoculture systems.

3.3.2. Brain tumors

The core challenge in high-throughput construction of brain tumor patient-derived organoids is that as bioink volume increases, it tends to contact the walls of multi-well plates, causing surface tension to collapse it into a two-dimensional culture. To address this issue, inspired by the freeform reversible embedding of suspended hydrogels printing method, an immersed bioprinting technology was developed to print organoids into a support bath within the plate wells. By using a hyaluronic acid solution as a protective support bath, contact between the organoids and the well walls is effectively blocked, preventing morphological distortion while ensuring more consistent volume and geometric shape of the printed organoids. Through this optimized method for drug screening of glioma and lung adenocarcinoma brain metastasis patient-derived organoids, researchers observed heterogeneity in the dose-dependent responses of these organoids to p53 activators and the commonly used clinical brain tumor drug temozolomide—p53 activators were effective in all patient-derived organoids, while temozolomide responses varied significantly due to the genetic and epigenetic characteristics of different tumors. This discovery reveals the strong potential of immersed bioprinting for automated manufacturing of patient-derived brain tumor organoids, laying a technical foundation for preclinical applications. However, the observed heterogeneity in drug responses highlights the need for extensive validation against actual patient outcomes to establish predictive performance for clinical use.[57] Taken together, immersion-based and spatially controlled printing strategies provide a scalable route to standardized brain tumor organoids with improved geometric consistency and screening utility. Their main value lies in bridging the gap between patient-derived heterogeneity and the need for reproducible high-throughput analysis.

3.4. Urinary system

3.4.1. Renal carcinoma

Traditional renal cell carcinoma (RCC) organoid technology often relies on Matrigel droplets, which involve tedious manual operations, large batch-to-batch variation, functional immaturity, and low throughput, seriously hindering drug-testing research on patient-specific heterogeneous clinical responses. Using bioprinting technology, researchers have successfully achieved the automated, stable construction and quality control of heterogeneous RCC organoids with uniform sizes in batches. These bioprinted RCC organoids not only retain the pathological morphology and gene mutation/expression characteristics of primary tumors but also exhibit inter-organoid and inter-patient heterogeneity even after long-term culture, providing an ideal model for preclinical patient-specific drug screening.[38] This breakthrough marks a significant step forward for 3D bioprinting in preclinical personalized treatment research for kidney cancer, particularly in accurately reflecting tumor heterogeneity. While these models are ideal for preclinical screening, their direct utility in guiding individual patient treatment decisions still requires robust clinical validation.

To further enhance the physiological relevance and functional complexity of kidney cancer organoid models, 3D bioprinting is evolving to integrate more complex cell types and construct multicellular tumor microenvironments. An innovative organ-on-a-chip platform has emerged, which uses granular microgels to construct neuronal networks and introduces organoids, including prostate cancer spheroids and patient-derived RCC organoids, through aspiration-assisted bioprinting to achieve innervation of various tissue types. This microfluidic device features an open tissue chamber for flexible manipulation and can accommodate microgels over 50 μm, providing flexibility for constructing customizable hydrogel microenvironments.[61] By reconstructing RCC cell aggregates with stromal components to form organized structures that reflect *in vivo* vascular morphology and spatial tumor microenvironment heterogeneity, 3D bioprinting not only deepens understanding of tumor physiological mechanisms but also offers broad prospects for developing preclinical models for personalized treatment methods.[38] These advances collectively demonstrate the powerful potential of 3D bioprinting in kidney cancer organoid model construction, moving from simulating a single tumor to integrating complex physiological functions. In renal carcinoma, the key advance is the move from manually variable Matrigel-based culture toward automated bioprinted systems with better size control, reproducibility, and heterogeneity retention. This progress is especially relevant for preclinical drug testing because renal tumors are highly heterogeneous and often show inconsistent treatment responses across patients.

3.4.2. Carcinoma of the bladder

In the era of precision medicine, quantifying intratumoral heterogeneity is crucial for developing effective treatment strategies. Researchers have used piezoelectric inkjet printing technology for the first time, providing a

revolutionary tool for analyzing intratumoral heterogeneity in bladder cancer. This method dissociates patient-derived tumor organoids into single-cell suspensions and, as bioink, precisely dispenses individual cells into microwell plates through on-demand inkjet printing without additives or processing. These single cells are then cultured into new organoids for further analysis. The study showed that these single-cell-derived organoids exhibited heterogeneous size, morphology, and expression of proliferation and apoptosis markers, and responded differently to chemotherapy drugs. By quantifying the mRNA expression levels of representative luminal and basal genes in different types of organoids, the heterogeneity of gene expression among individual organoids was further confirmed. The study demonstrates that fully automated inkjet printing technology can serve as an effective tool for cell sorting and in-depth assessment of intratumoral heterogeneity in bladder cancer, providing a new research path for the preclinical design of personalized treatment strategies. However, the clinical utility of these models in directly informing treatment decisions requires further prospective validation in clinical settings.[60] The work highlights the unique advantage of inkjet-based bioprinting for single-cell resolution studies of intratumoral heterogeneity. By enabling the controlled rebuilding of organoids from dissociated patient-derived cells, this approach offers a practical framework for dissecting phenotypic diversity and refining personalized treatment strategies in bladder cancer.

3.5. Respiratory system

Despite rapid advances in *in vitro* cancer models, models that can simultaneously reproduce the complexity, diverse cellular components, and genetic characteristics of the tumor microenvironment are still lacking. Bioprinting technology offers a new approach to building more accurate lung cancer models. Researchers proposed an advanced vascularized lung cancer model that integrates patient-derived lung cancer organoids (LCOs), lung fibroblasts, and perfusable blood vessels through 3D bioprinting. To more realistically simulate the biochemical composition of native lung tissue, the model uses porcine lung-derived decellularized extracellular matrix hydrogel, providing physical and biochemical signals for cells in the lung cancer microenvironment. Notably, the model introduces idiopathic pulmonary fibrosis-derived lung fibroblasts to simulate human fibrotic lesions. In a fibrotic environment, both cell proliferation and drug resistance-related LCO gene expression increased. More importantly, compared with Matrigel, LCOs with fibrosis constructed in lung-derived decellularized extracellular matrix showed greater changes in sensitivity to targeted anticancer drugs. This means this vascularized lung cancer model, capable of simulating lung fibrosis, can more accurately evaluate drug responses, thereby informing the development of appropriate preclinical models for lung cancer patients with pulmonary fibrosis. In the future, this method is expected to be applied to developing targeted treatment strategies or discovering biomarkers for lung cancer patients with fibrosis[62] (Figure 7A). These lung cancer models demonstrate that bioprinting can incorporate stromal and disease-specific components, such as fibrosis-associated fibroblasts and decellularized lung matrix, to improve the physiological relevance of drug-response testing. This is an important step toward modeling clinically meaningful subtypes of lung cancer rather than treating the disease as a uniform entity.

3.6. Endocrine system

Intertumoral heterogeneity in thyroid cancer poses a significant challenge for precision therapy, and traditional organoid models have limitations in efficiency and physiological relevance. Researchers developed droplet-engineered organoids (DEOs) using microfluidic 3D bioprinting technology to rapidly construct patient-derived thyroid cancer models. These DEOs can be generated within 10 days, demonstrating exceptional uniformity (coefficient of variation of only 2.54%) and a success rate as high as 76%. They not only faithfully reproduce the histopathological structure, genomic landscape (92% consistency in driver genes), and native immune microenvironment ($CD3^+$/$CD56^+$/$CD68^+$/alpha-smooth muscle $actin^+$) of the primary tumor, but also reveal patient-specific heterogeneity through drug screening, accurately reflecting clinical responses, including cisplatin sensitivity and resistance to programmed cell death protein 1 inhibitors.

Furthermore, researchers established a novel co-culture model of thyroid cancer and lung organoids to study the mechanisms of thyroid cancer lung metastasis. Through transcriptomic analysis, they discovered that the nuclear factor kappa B signaling pathway drives stage-specific maturation of thyroid cancer. Pharmacological inhibition of nuclear factor kappa B can synergistically enhance the efficacy of dasatinib, anti-programmed cell death protein 1, and paclitaxel, with combination index values of 0.58, 0.45, and 0.80, respectively. This indicates that the microfluidic 3D bioprinting platform provides a scalable, physiologically relevant tool for high-fidelity, rapid modeling of thyroid cancer, demonstrating strong translational potential for mechanistic research, drug screening, and preclinical personalized treatment evaluation63 (Figure 7B–E). However, it is crucial to distinguish retrospective correlations between drug

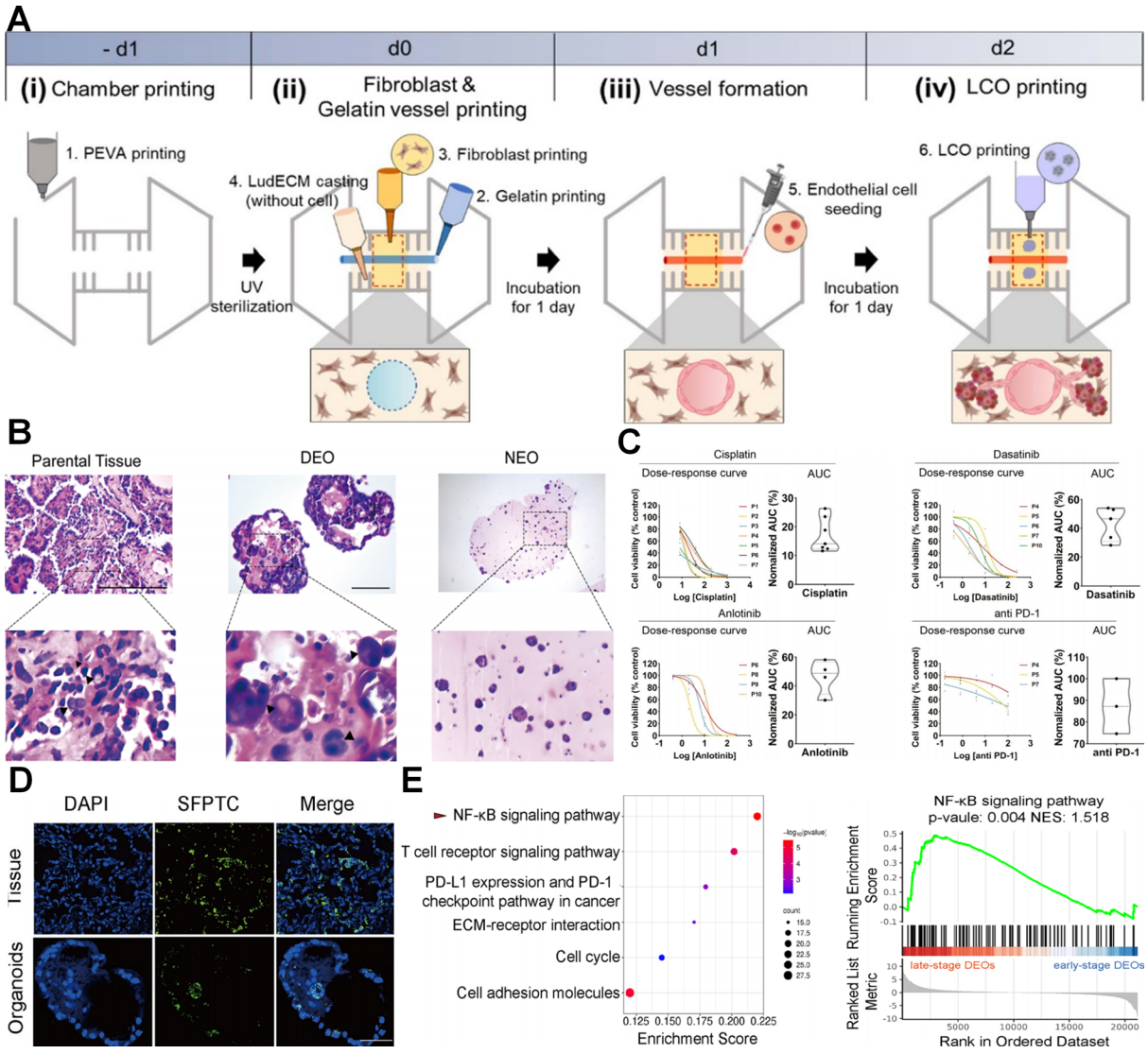


Figure 7. 3D bioprinted lung cancer and thyroid cancer organoid models. (A) Production and drug testing of a vascularized organoid model of lung cancer by 3D bioprinting. Reprinted with permission from Choi *et al.*[62] Copyright © 2023 IOP Publishing Ltd. (B) H&E staining of peritumoral tissue and DEO and NEO on day 10. Black arrows show clear cytoplasm with tumor tissue and DEO. (C) Different drug responses of patient-derived DEOS under drug treatment. Through high-throughput drug sensitivity detection, it was verified that patient-derived thyroid cancer DEOs generated by microfluidic 3D bioprinting can accurately capture patient-specific drug response heterogeneity. (D) Representative immunofluorescence images of SFPTC in parental lung tissue and DEOS. Nuclei were stained with DAPI (blue). (E) Scatter plot of KEGG pathway enrichment analysis of DEGS in DEOS on day 5 and day 10 (left). DGSEA in RNA-SEQ data of early organoids and late organoids (right). Through multi-level transcriptomics analysis, the stage-specific maturation of DEOs in thyroid cancer driven by the NF-κB signaling pathway was revealed, which laid a solid molecular foundation for the subsequent synergistic treatment strategy of NF-κB inhibition combined with antitumor drugs. Reprinted from Gao *et al.*[63]

responses in these models and clinical responses from the prospective predictive performance needed to guide individualized clinical treatment. Comprehensive clinical validation, including defined patient numbers, validation designs, and predictive performance metrics, is still needed to establish direct clinical utility. Recent thyroid cancer studies show that microfluidic bioprinting can support rapid organoid generation while preserving driver gene profiles, immune features, and patient-specific therapeutic responses. This combination of speed, reproducibility, and biological fidelity makes the platform particularly promising for translational research in a tumor type with marked interpatient heterogeneity (Table 3).

Table 3. Performance comparison of *in vitro* tumor models constructed by different three-dimensional bioprinting methods

Printing method/ configuration strategy	Extrusion bioprinting	Gel jetting/piezoelectric inkjet printing	Photocuring/projection-based printing	Laser-induced forward transfer/ laser-induced/non-contact deposition	Microfluidic assembly/ chip-based platforms	Hybrid strategy (printed channels + gel perfusion/ cell spheroid formation/ re-curing; or post-print deposition)
Channel connectivity success rate	Channels often depend on gel rheology and support structures; clear connectivity is usually achievable, but is susceptible to shrinkage/ collapse	Droplet deposition can form microstructures, but connected channels require additional design (post-processing or channel formation)	High structural precision: channel geometry can be accurately defined, but connectivity stability depends on shrinkage and material post-processing	Mostly used for precise deposition of cell/ biomaterial patterns; channel connectivity usually requires secondary shaping	Channels are inherently microfluidic networks, so connectivity is strong	Printing handles geometry, while perfusion handles filling and connectivity, often improving stability
Tumor spheroid formation success rate	Cells and matrix can be guided to remodel along printed paths to form spheroids/clusters; however, the parameter window is broad	When driven by cell aggregates/microdroplets: microdroplet deposition can promote local cell aggregation; however, cluster size and uniformity are affected by droplet dynamics	If cells are nucleated directly during printing or encapsulated during printing, spheroid formation depends on the material environment; cell viability is more sensitive	Patterned deposition facilitates tissue-like structure formation	Clusters/organoid-like structures can be formed through flow-field shear, phase separation, or gradient nucleation	Cells can be aggregated and matured under milder conditions
Cell viability (range expression)	Generally relatively mild, but shear and residence time matter; literature often reports this as a range of "maintained viability with batch-to-batch variation"	Usually low thermal/photo stress; however, jetting acceleration/shear and droplet nucleation can still cause differences	Light/free radicals/ crosslinking byproducts may affect cells; with low-toxicity formulations, optimized light dose, and post-processing to remove residues, performance can improve to moderate or better	Medium to high: non-contact operation reduces mechanical shear, but laser energy and thermal effects, together with target material absorption, determine cell outcomes	Relatively mild: shear is controllable, but local shear peaks and culture medium composition determine survival	Reduces direct damage during printing, allowing spheroid formation to occur under gentle culture conditions
Reproducibility (equipment accessibility/ formulation consistency)	Equipment threshold is relatively accessible; formulation consistency is critical (viscosity, crosslinking kinetics, particle/precursor stability), which determines batch-to-batch variation	Equipment is accessible in some labs; however, ink surface tension, viscosity, particle content, and stability determine reproducibility	Equipment threshold is medium-to-high; material formulation consistency is critical (photoinitiator, crosslinking degree, residue removal)	Low to medium: high equipment threshold; formulation window may also be narrow	Chip fabrication threshold depends on the process (soft lithography/molding); batch consistency mainly depends on the preparation workflow	Combined processes are more complex and have more parameters, but key steps can be consolidated

(*Cont'd...*)

Table 3. (*Continued*)

Printing method/ configuration strategy	Extrusion bioprinting	Gel jetting/piezoelectric inkjet printing	Photocuring/projection-based printing	Laser-induced forward transfer/ laser-induced/non-contact deposition	Microfluidic assembly/ chip-based platforms	Hybrid strategy (printed channels + gel perfusion/ cell spheroid formation/ re-curing; or post-print deposition)
Technical feasibility (resolution-throughput, ink requirements, assembly gentleness)	Ink must be adapted: viscosity window + controllable crosslinking/ curing; assembly is usually gentle (shear is the main source of damage)	Microscale droplets, but throughput and continuity are affected by nozzle count and ink supply; requires more print-friendly inks	High resolution and geometric throughput; however, high requirements for bioinks, photoinitiation systems, and cell compatibility; assembly gentleness depends on the curing strategy	High resolution, but throughput is often limited by writing speed; requires absorbers/material engineering; assembly is generally gentle (non-contact)	High resolution, controllable throughput but not always high; cell-friendly; requires compatibility with culture medium systems	Resolution depends on the printed portion versus increased assembly steps; ink requirements can be decoupled
Drug screening performance (gradient / high throughput)	Gradient: depends on perfusion/microfluidic integration; high throughput: parallel devices must be designed	Gradient: if a drug diffusion gradient is needed, external perfusion/ microfluidic coupling is often required. High throughput: suitable for arraying, but still limited by culture/detection channels	Gradient: precise channels enable controlled perfusion gradients; high throughput: arrayed chips/ culture plate coupling is more suitable	High throughput: difficult to rapidly write large-scale arrays	Gradient: microfluidics excels at controlled spatiotemporal gradients; high throughput: can be achieved with parallel chips/multichannel devices	Gradient: channels + perfusion are very useful; high throughput: depends on the degree of parallelization/automation
Main advantages	Programmable structure, integrated channels/ tumor regions, and good compatibility with multiple materials	Suitable for "arrayed tumor micro-spheroids" and medium-scale screening; avoids complex support structures	High precision, scalable fabrication, and channel-friendly design	Excellent ultrafine patterning and cell-position control	Strongest capability for gradient generation and dose control; suitable for mechanistic studies and pharmacodynamic characterization	More balanced: separates "structural precision" from "cell friendliness"
Main limitations	Resolution is limited; shear/nozzle clogging and batch variation are issues; cell migration and cluster maturation may take longer	Channel connectivity is weaker than integrated extrusion printing; narrow ink window and nozzle clogging risk; long-term structural stability requires material-system support	Biocompatibility challenges (photo/ chemical crosslinking); material post-processing adds complexity	Cost and throughput limitations; more oriented toward configuration studies than large-scale drug screening platforms	Increased structural complexity; integration with printing often requires additional engineering; scaling to large-scale screening still requires system-level work	Longer process chain; greater difficulty in standardization and automation

doi: 10.36922/IJB026400430

4. Challenges and perspectives

4.1. Unique advantages of three-dimensional bioprinting in constructing *in vitro* tumor models

Three-dimensional bioprinting technology has demonstrated significant advantages in constructing *in vitro* tumor models, offering unique value that traditional methods struggle to match. First, this technology can precisely control the spatial distribution and organizational structure of cells, accurately regulating cell types, cell density, and biomatrix components, making the constructed tumor models closer to the histological characteristics of *in vivo* tumors and more realistically reproducing the complex interactions between multiple cell types within the tumor microenvironment. Second, 3D-printed tumor organoids offer high reproducibility and standardization, significantly reducing operational variability in traditional manual construction and enabling high-throughput, automated, uniform batch manufacturing. Third, cells in these organoids exist in a 3D space, facing nutrient, oxygen, and intercellular signaling molecule concentration gradients that more closely match *in vivo* physiological conditions, thereby better reflecting tumor cell behavior. Finally, by integrating analytical technologies such as genetic analysis, transcriptomic analysis, and drug screening, 3D-printed tumor organoids can accurately evaluate drug responses, reveal drug-resistance mechanisms, and predict clinical efficacy, providing strong support for individualized treatment and precision medicine.

4.2. Patient-level limitations and validation challenges

Although 3D bioprinted tumor organoids have made significant progress in in vitro model construction, several patient-level limitations and validation challenges must be addressed to achieve clinical application. First, significant differences exist between *in vitro* models and clinical patients. Although correlations have been shown between *in vitro* drug sensitivity data and clinical efficacy in some patients, validation through rigorous prospective clinical trials is still required. Second, the complex microenvironment of *in vivo* tumors, including complete vascular systems, complex immune cell infiltration, dynamic cytokine gradients, and time-related physiological changes, remains difficult to fully reproduce i*n vitro* models. Therefore, individual predictive performance assessments based on these models may not be sufficient to guide clinical treatment decisions and should be combined with other diagnostic methods and clinical evidence to establish their true clinical utility.

4.3. Key requirements for clinical translation

Key steps in translating from *in vitro* models to clinical application include systematic requirements across multiple aspects. First, prospective clinical validation is essential and should include sufficient patient cohort sizes, well-defined validation designs, and clear predictive performance indicators. Second, a standardized drug response assessment framework needs to be established, including unified drug concentration ranges, functional readout indicators, data quality control standards, and cross-center testing methods. Third, integration with existing diagnostic workflows is crucial; bioprinted models should be coordinated with existing clinical diagnostic methods such as imaging, pathology, and molecular testing. Fourth, translational manufacturing and regulatory hurdles must be resolved, including Good Manufacturing Practice certification, large-scale production process validation, immunogenicity assessment, safety and efficacy regulatory requirements, and regulatory coordination across countries and regions. In addition, intellectual property protection, cost-benefit assessment, and clinical acceptability evaluation are also important factors to ensure successful clinical translation. These comprehensive requirements indicate that the transition from laboratory technology to clinical application tools will be a long-term, complex process requiring multidisciplinary collaboration.

4.4. Prospects for multicellular interactions and functional relevance

Although many studies have integrated multiple components such as mesenchymal cells, extracellular matrix components, immune cells, and vessel-like structures into printed constructs, the functional interactions and biological relevance of these components still require further in-depth discussion. Structural similarity does not equate to functional biological relevance. For example, while printing systems may morphologically contain vessel-like structures, whether they can truly achieve vascular functions, maintain complete oxygen and nutrient gradients, support immune cell migration and function, and promote functions such as dynamic remodeling of the extracellular matrix remains a key issue. Future research should focus on distinguishing between the following aspects: (i) the difference between physical assembly and functional synergy of multiple cell types; (ii) the relationship between the simulation accuracy of nutrient/oxygen gradients and cellular physiological responses; (iii) the difference between the degree of immune cell infiltration and the actual performance of immune functions; (iv) the degree of correlation

between extracellular matrix similarity and its dynamic biological activity. Such in-depth functional analysis will help researchers and clinicians better understand the true biological significance of printed organoids for drug resistance research and immunotherapy response prediction, advancing precision oncology.

5. Conclusion

Complexity and heterogeneity make it difficult for traditional two-dimensional cultures and animal models to accurately simulate the *in vivo* tumor microenvironment. This review systematically summarizes the latest progress of 3D bioprinting technology in tumor organoid construction, focusing on the principles, advantages, and limitations of extrusion-based, inkjet-based, and lithography-based bioprinting methods. The review introduces in detail application examples of this technology in tumors of multiple systems, such as the digestive system (colon cancer, gastric cancer, pancreatic cancer), reproductive system (breast cancer), nervous system (glioma), urinary system, respiratory system (lung cancer), and endocrine system (thyroid cancer), demonstrating the application potential of this technology in drug screening, tumor heterogeneity research, and individualized precision medicine. 3D bioprinting provides new tools for oncology and precision medicine research by precisely controlling cell spatial distribution, improving model reproducibility, creating more complex microenvironment gradients, and integrating multi-dimensional analytical techniques. Although the technology has achieved major breakthroughs in many areas, the transition from a basic research tool to a clinical decision-support tool still requires more basic research and clinical validation. By deepening multicellular interaction models, optimizing bioink formulations, strengthening prospective clinical validation, and addressing key manufacturing and regulatory obstacles, 3D bioprinted tumor organoids are expected to gradually advance precision oncology and individualized cancer treatment.

Acknowledgments

None.

Funding

None.

Conflict of interest

The authors declare that they have no known competing financial interests or personal relationships that could have appeared to influence the work reported in this paper.

Author contributions

Conceptualization: Zhiyan Zhang, Tingyu Wang
Supervision: Zhiyan Zhang, Bo Qiao
Visualization: Zhiyan Zhang, Xiangran Cui
Writing–original draft: Zhiyan Zhang, Shuo Wu
Writing–review & editing: Zhiyan Zhang, Guoliang Zheng

Ethics approval and consent to participate

Not applicable.

Consent for publication

Not applicable.

Availability of data

Not applicable.

References

1. Filho AM, Laversanne M, Ferlay J, *et al*. The GLOBOCAN 2022 cancer estimates: data sources, methods, and a snapshot of the cancer burden worldwide. *Int J Cancer*. 2025;156(7):1336-1346.

   doi: 10.1002/ijc.35278

2. Zhang L, Zheng H, Jiang ST, *et al*. Worldwide research trends on tumor burden and immunotherapy: a bibliometric analysis. *Int J Surg*. 2024;110(3):1699-1710.

   doi: 10.1097/JS9.0000000000001022

3. Zhou BL, Zang RC, Zhang MY, *et al*. Worldwide burden and epidemiological trends of tracheal, bronchus, and lung cancer: a population-based study. *EBioMedicine*. 2022;78:103951.

   doi: 10.1016/j.ebiom.2022.103951

4. Xiang DH, Hu SW, Mai TX, *et al*. Worldwide cancer statistics of adults over 75 years old in 2019: a systematic analysis of the global burden of disease study 2019. *BMC Public Health*. 2022;22(1):1979.

   doi: 10.1186/s12889-022-14412-1

5. Yu Q, Zhang YF, Qiao L, *et al*. The evolving global burden of kidney cancer: a comparative analysis of trends in China and worldwide with projections to 2041. *Urol Oncol*. 2026;44(7):280-296.

   doi: 10.1016/j.urolonc.2026.03.005

6. Crucitta S, Cucchiara F, Mathijssen R, *et al*. Treatment-driven tumour heterogeneity and drug resistance: lessons from solid tumours. *Cancer Treat Rev*. 2022;104:102340.

   doi: 10.1016/j.ctrv.2022.102340

7. Kou ZX, Liu C, Zhang WF, Sun CG, Liu LJ, Zhang QM. Heterogeneity of primary and metastatic CAFs: from differential treatment outcomes to treatment opportunities

(review). *Int J Oncol*. 2024;64(5):54.

doi: 10.3892/ijo.2024.5642

8. Zhang XY, Xie JJ, Yang ZX, Yu CKW, Hu YH, Qin J. Tumour heterogeneity and personalized treatment screening based on single-cell transcriptomics. *Comput Struct Biotechnol J*. 2025;27:307-320.

doi: 10.1016/j.csbj.2024.12.020

9. Huang JB, Wang HY, Jiang DH, *et al*. Development of novel PROTAC RAD51 degraders as enhancers of DNA damage response for hepatocellular carcinoma treatment. *J Med Chem*. 2026;69(4):3957-3983.

doi: 10.1021/acs.jmedchem.5c02624

10. Jose A, Kulkarni P, Thilakan J, *et al*. Integration of pan-omics technologies and three-dimensional in vitro tumor models: an approach toward drug discovery and precision medicine. *Mol Cancer*. 2024;23(1):50.

doi: 10.1186/s12943-023-01916-6

11. Song SL, Li B, Carvalho MR, *et al*. Complex in vitro 3D models of digestive system tumors to advance precision medicine and drug testing: progress, challenges, and trends. *Pharmacol Ther*. 2022;239:108276.

doi: 10.1016/j.pharmthera.2022.108276

12. Wang LM, Hu DP, Xu JM, Hu J, Wang YF. Complex in vitro model: a transformative model in drug development and precision medicine. *Clin Transl Sci*. 2024;17(2):e13695.

doi: 10.1111/cts.13695

13. Wan LFY, Zhao YJ, Huang C, *et al*. Carbazole/triphenylamine-based red-emitting probes for mitochondrial viscosity imaging and tumor visualization. *J Photochem Photobiol A Chem*. 2026;478:117253.

doi: 10.1016/j.jphotochem.2026.117253

14. Deng Y, Zhao XY, Su Q, *et al*. Application of a near-infrared fluorescent probe with dual-targeting capability toward lipid droplets and mitochondria in imaging of liver cirrhosis and tumors. *Spectrochim Acta A Mol Biomol Spectrosc*. 2026;353:127593.

doi: 10.1016/j.saa.2026.127593

15. Chawla U, Dahiya D, Kumar Y, *et al*. A review on ZnO-based targeted drug delivery system. *Lett Drug Des Discov*. 2024;21(3):397-420.

doi: 10.2174/1570180820666230222092950

16. Bini F, D'Alessandro S, Agarwal T, *et al*. Biomimetic 3D bioprinting approaches to engineer the tumor microenvironment. *Int J Bioprint*. 2023;9(6):1022.

doi: 10.36922/ijb.1022

17. Datta P, Dey M, Ataie Z, Unutmaz D, Ozbolat IT. 3D bioprinting for reconstituting the cancer microenvironment. *NPJ Precis Oncol*. 2020;4(1):18.

doi: 10.1038/s41698-020-0121-2

18. Shukla P, Yeleswarapu S, Heinrich MA, Prakash J, Pati F. Mimicking tumor microenvironment by 3D bioprinting: 3D cancer modeling. *Biofabrication*. 2022;14(3):032002.

doi: 10.1088/1758-5090/ac6d11

19. Chen H, Wu ZH, Gong ZY, *et al*. Acoustic bioprinting of patient-derived organoids for predicting cancer therapy responses. *Adv Healthc Mater*. 2022;11(13):2102784.

doi: 10.1002/adhm.202102784

20. Samadian H, Jafari S, Sepand MR, *et al*. 3D bioprinting technology to mimic the tumor microenvironment: tumor-on-a-chip concept. *Mater Today Adv*. 2021;12:100160.

doi: 10.1016/j.mtadv.2021.100160

21. Xu KL, Huang YY, Wu MB, Yin J, Wei P. 3D bioprinting of multi-cellular tumor microenvironment for prostate cancer metastasis. *Biofabrication*. 2023;15(3):035020.

doi: 10.1088/1758-5090/acd960

22. D'Alessandro S, Mohammadi S, Iafrate L, *et al*. Hybrid 3D microfluidic bioprinting for the engineering of cancer models and tissue substitutes. *Virtual Phys Prototyp*. 2024;19(1):e2419411.

doi: 10.1080/17452759.2024.2419411

23. Lee G, Kim SJ, Park JK. Fabrication of a self-assembled and vascularized tumor array via bioprinting on a microfluidic chip. *Lab Chip*. 2023;23(18):4079-4091.

doi: 10.1039/d3lc00275f

24. Radhakrishnan J, Varadaraj S, Dash SK, Sharma A, Verma RS. Organotypic cancer tissue models for drug screening: 3D constructs, bioprinting and microfluidic chips. *Drug Discov Today*. 2020;25(5):879-890.

doi: 10.1016/j.drudis.2020.03.002

25. Sibbitts J, Di Pietro L, Privitera A, *et al*. 3D bioprinting and microfluidic-based devices for cancer detection and drug treatment: focus on prostate cancer. *Curr Med Chem*. 2026;33(8):1503-1522.

doi: 10.2174/0109298673298382240307040239

26. Pellegrino P, Greco S, Gonzàlez AD, *et al*. Establishment of 3D cultures of myometrium, leiomyoma, and leiomyosarcoma cells: advantages and disadvantages of two different models. *Reprod Sci*. 2024;31(12):3729-3742.

doi: 10.1007/s43032-024-01724-3

27. Thibieroz N, Picart C, Migliorini E. Advanced biomaterial strategies for 3D in vitro biomimetic neuroblastoma cell culture. *Biomater Sci*. 2026;14(17):4418-4434.

doi: 10.1039/d6bm00438e

28. Cui XR, Jiao JH, Yang LL, *et al*. Advanced tumor organoid bioprinting strategy for oncology research. *Mater Today Bio*. 2024;28:101198.

doi: 10.1016/j.mtbio.2024.101198

29. Dai R, Chen W, Chen Y, *et al*. 3D bioprinting platform development for high-throughput cancer organoid models construction and drug evaluation. *Biofabrication*. 2024;16(3):035026.

doi: 10.1088/1758-5090/ad51a6

30. Han J, Jeong HJ, Choi J, *et al*. Bioprinted patient-derived organoid arrays capture intrinsic and extrinsic tumor features for advanced personalized medicine. *Adv Sci (Weinh)*. 2025;12(20):2407871.

doi: 10.1002/advs.202407871

31. Dong QQ, Su X, Li X, *et al*. In vitro construction of lung cancer organoids by 3D bioprinting for drug evaluation. *Colloids Surf A Physicochem Eng Asp*. 2023;666:131288.

doi: 10.1016/j.colsurfa.2023.131288

32. Pérez-Pedroza R, Al-Jalih F, Xu JY, Moretti M, Briola GR, Hauser CAE. Fabrication of lumen-forming colorectal cancer organoids using a newly designed laminin-derived bioink. *Int J Bioprint*. 2022;9(1):633.

doi: 10.18063/ijb.v9i1.633

33. Wang Q, Yuan FW, Zuo XL, Li M. Breakthroughs and challenges of organoid models for assessing cancer immunotherapy: a cutting-edge tool for advancing personalised treatments. *Cell Death Discov*. 2025;11(1):222.

doi: 10.1038/s41420-025-02505-w

34. Ju MG, Jin ZZ, Yu X, *et al*. Gastric cancer models developed via GelMA 3D bioprinting accurately mimic cancer hallmarks, tumor microenvironment features, and drug responses. *Small*. 2025;21(8):2409321.

doi: 10.1002/smll.202409321

35. Tebon PJ, Wang B, Markowitz AL, *et al*. Drug screening at single-organoid resolution via bioprinting and interferometry. *Nat Commun*. 2023;14(1):3168.

doi: 10.1038/s41467-023-38832-8

36. Tong F, Nie RJ, Wu ZY, *et al*. Construction of 3D bioprinted colorectal cancer models and evaluation of their efficacy and drug sensitivity. *APL Bioeng*. 2026;10(3):036106.

doi: 10.1063/5.0320497

37. Du LW, Zheng ZC, Zhang K, *et al*. Exploring personalized prediction of clinical chemotherapy efficacy and revealing tumor heterogeneity using patient-derived 3D bioprinting gastric cancer models. *Mol Cancer*. 2025;24(1):259.

doi: 10.1186/s12943-025-02466-9

38. Mao SS, Xie RY, Shou JZ, Pang Y, Sun W. Bioprinting of patient-derived heterogeneous renal cell carcinoma organoids for personalized therapy. *Biofabrication*. 2025;17(4):045008.

doi: 10.1088/1758-5090/adecc5

39. Mu PY, Zhou SJ, Lv T, *et al*. Newly developed 3D in vitro models to study tumor-immune interaction. *J Exp Clin Cancer Res*. 2023;42(1):81.

doi: 10.1186/s13046-023-02653-w

40. Li H, Jin CR. Retinoblastoma: unveiling molecular pathogenesis and pioneering organoid-driven therapeutic innovations. *Stem Cell Res Ther*. 2026;17(1):96.

doi: 10.1186/s13287-026-04951-4

41. Maloney E, Clark C, Sivakumar H, *et al*. Immersion bioprinting of tumor organoids in multi-well plates for increasing chemotherapy screening throughput. *Micromachines (Basel)*. 2020;11(2):208.

doi: 10.3390/mi11020208

42. Wen J, Liu FK, Cheng Q, *et al*. Applications of organoid technology to brain tumors. *CNS Neurosci Ther*. 2023;29(10):2725-2743.

doi: 10.1111/cns.14272

43. Feng SJ, Zhang Y, Wang YY, Gao YF, Song YJ. Harnessing gene editing technology for tumor microenvironment modulation: an emerging anticancer strategy. *Chemistry*. 2024;30(62):e202402485.

doi: 10.1002/chem.202402485

44. Wang ZH, Guo LY, Li Z, *et al*. Three-dimensional fluorescence spectroscopy recognition and component analysis based on machine learning. *Spectrochim Acta A Mol Biomol Spectrosc*. 2026;354:127633.

doi: 10.1016/j.saa.2026.127633

45. Fan YP, Zhang YT, Zhang GY, *et al*. Proteomic profiling of urinary large extracellular vesicles for the diagnosis of prostate cancer. *Anal Chem*. 2025;97(32):17368-17379.

doi: 10.1021/acs.analchem.5c01320

46. Molander D, Sbirkov Y, Bodurov I, Dikov D, Sarafian V. Comparative analysis of bioinks in 3D bioprinted organoids of colorectal cancer. *Acta Morphol Anthropol*. 2022;29(3-4).

doi: 10.7546/ama.29.3-4.2022.03

47. Chen H, Du L, Li J, *et al*. Modeling cancer metastasis using acoustically bio-printed patient-derived 3D tumor microtissues. *J Mater Chem B*. 2022;10(11):1843-1852.

doi: 10.1039/d1tb02789a

48. Wang PP, Sun LJ, Li CC, *et al*. Study on drug screening multicellular model for colorectal cancer constructed by three-dimensional bioprinting technology. *Int J Bioprint*. 2023;9(3):379-398.

doi: 10.18063/ijb.694

49. McGuckin C, Forraz N, Milet C, *et al*. Stable biotherapeutic penetration screening in critically small colorectal metastatic cancer biopsies allows for oncolytic virus-delivered chemotherapeutic response assessment through

3D bioprinted organoid expansion. *Adv Ther (Weinh)*. 2025;8(1):2400221.

doi: 10.1002/adtp.202400221

50. Hou S, Tiriac H, Sridharan BP, *et al*. Advanced development of primary pancreatic organoid tumor models for high-throughput phenotypic drug screening. *SLAS Discov*. 2018;23(6):574-584.

doi: 10.1177/2472555218766842

51. Fernandez-Vega V, Hou S, Plenker D, *et al*. Lead identification using 3D models of pancreatic cancer. *SLAS Discov*. 2022;27(3):159-166.

doi: 10.1016/j.slasd.2022.03.002

52. Reid JA, Palmer XL, Mollica PA, Northam N, Sachs PC, Bruno RD. A 3D bioprinter platform for mechanistic analysis of tumoroids and chimeric mammary organoids. *Sci Rep*. 2019;9(1):97466.

doi: 10.1038/s41598-019-43922-z

53. Mollica PA, Booth-Creech EN, Reid JA, *et al*. 3D bioprinted mammary organoids and tumoroids in human mammary derived ECM hydrogels. *Acta Biomater*. 2019;95:201-213.

doi: 10.1016/j.actbio.2019.06.017

54. Shi W, Mirza S, Kuss M, *et al*. Embedded bioprinting of breast tumor cells and organoids using low-concentration collagen-based bioinks. *Adv Healthc Mater*. 2023;12(26).

doi: 10.1002/adhm.202300905

55. Bjerring JS, Khodour Y, Peterson EA, Sachs PC, Bruno RD. Intercellular mitochondrial transfer contributes to microenvironmental redirection of cancer cell fate. *FEBS J*. 2025;292(9):2306-2322.

doi: 10.1111/febs.70002

56. van Pel DM, Harada K, Song D, Naus CC, Sin WC. Modelling glioma invasion using 3D bioprinting and scaffold-free 3D culture. *J Cell Commun Signal*. 2018;12(4):723-730.

doi: 10.1007/s12079-018-0469-z

57. Clark CC, Yoo KM, Sivakumar H, *et al*. Immersion bioprinting of hyaluronan and collagen bioink-supported 3D patient-derived brain tumor organoids. *Biomed Mater*. 2023;18(1):015014.

doi: 10.1088/1748-605X/aca05d

58. Tang M, Xie Q, Gimple RC, *et al*. Three-dimensional bioprinted glioblastoma microenvironments model cellular dependencies and immune interactions. *Cell Res*. 2020;30(10):833-853.

doi: 10.1038/s41422-020-0338-1

59. Roth JG, Brunel LG, Huang MS, *et al*. Spatially controlled construction of assembloids using bioprinting. *Nat Commun*. 2023;14(1):4300.

doi: 10.1038/s41467-023-40006-5

60. Yoon WH, Lee HR, Kim S, *et al*. Use of inkjet-printed single cells to quantify intratumoral heterogeneity. *Biofabrication*. 2020;12(3):035030.

doi: 10.1088/1758-5090/ab9491

61. Fredrikson JP, Roth DM, Cosgrove JA, *et al*. Engineering neuronal networks in granular microgels to innervate bioprinted cancer organoids on-a-chip. *Lab Chip*. 2025;25(14):3467-3481.

doi: 10.1039/d5lc00134j

62. Choi YM, Lee H, Ann M, Song M, Rheey J, Jang J. 3D bioprinted vascularized lung cancer organoid models with underlying disease capable of more precise drug evaluation. *Biofabrication*. 2023;15(3):034104.

doi: 10.1088/1758-5090/acd95f

63. Gao H, Lin J, Chen X, *et al*. Microfluidic-based patient-derived organoids recapitulate thyroid cancer heterogeneity and reveal NF-κB-driven maturation for precision therapy. *J Transl Med*. 2026;24(1):467.

doi: 10.1186/s12967-026-07882-z

64. Zelaia Amilibia M, Aizarna-Lopetegui U, Sánchez LP, *et al*. Novel printing strategy for high fidelity extrusion-based bioprinted multi-material nested models. *Biomed Mater*. 2026;21(3):035019.

doi: 10.1088/1748-605X/ae6aea

65. Ding J, Li YY, Wu Y, Xu JB, Huang ZW, Huang B. Optimized design of a multichannel integrated nozzle for extrusion-based 3D bioprinting: balancing cell viability and printing precision. *Rapid Prototyp J*. 2026:1-19.

doi: 10.1108/RPJ-01-2026-0020

66. Li JF, Fischer P. Advances in extrusion-based bioprinting enabled by advanced printhead and nozzle designs. *Mater Today Bio*. 2026;37:102941.

doi: 10.1016/j.mtbio.2026.102941

67. Zhang T, Zhao W, Zijie XH, Wang XW, Zhang KX, Yin JB. Bioink design for extrusion-based bioprinting. *Appl Mater Today*. 2021;25:101227.

doi: 10.1016/j.apmt.2021.101227

68. Cui RW, Li SM, Li TY, *et al*. Natural polymer derived hydrogel bioink with enhanced thixotropy improves printability and cellular preservation in 3D bioprinting. *J Mater Chem B*. 2023;11(17):3907-3918.

doi: 10.1039/d2tb02786k

69. Leucht A, Volz AC, Rogal J, Borchers K, Kluger PJ. Advanced gelatin-based vascularization bioinks for extrusion-based bioprinting of vascularized bone equivalents. *Sci Rep*. 2020;10(1):5330.

doi: 10.1038/s41598-020-62166-w

70. Wei LC, Li Z, Li JJ, *et al*. An approach for mechanical property

optimization of cell-laden alginate-gelatin composite bioink with bioactive glass nanoparticles. *J Mater Sci Mater Med*. 2020;31(11):103.

doi: 10.1007/s10856-020-06440-3

71. Le H, Tran ATT, Waheed A, Tung TT, Losic D. Extrusion bioprinting for wound healing: innovations in functionalized bioinks and bioprinting technology. *Adv Mater Technol*. 2026;11(18).

doi: 10.1002/admt.71143

72. Naolou T, Schadzek N, Nolte J, *et al*. Additive-free hyaluronic acid-based bioink for 3D bioprinting of bone marrow microenvironments. *Mater Today Bio*. 2025;35:102512.

doi: 10.1016/j.mtbio.2025.102512

73. Al Qassab M, Merheb M, Sayadi S, *et al*. Organ-specific strategies in bioprinting: addressing translational challenges in the heart, liver, kidney, and pancreas. *J Funct Biomater*. 2025;16(10):356.

doi: 10.3390/jfb16100356

74. Borgia C, Gagliardi F, Gabriele D, Ambrogio G, Filice L. Bioinks for extrusion-based bioprinting: a systematic review of rheology, applications and future directions. *J Mech Sci Technol*. 2026;40(3):2379-2401.

doi: 10.1007/s12206-026-0267-0

75. Gao ZQ, Liu X, Zhao H, *et al*. Synthesis of easily-processable collagen bio-inks using ionic liquid for 3D bioprinted liver tissue models with branched vascular networks. *Sci China Chem*. 2023;66(5):1489-1499.

doi: 10.1007/s11426-022-1472-6

76. Horder H, Lasheras MG, Grummel N, *et al*. Bioprinting and differentiation of adipose-derived stromal cell spheroids for a 3D breast cancer-adipose tissue model. *Cells*. 2021;10(4):803.

doi: 10.3390/cells10040803

77. Wu T, Gao YY, Su J, *et al*. Three-dimensional bioprinting of artificial ovaries by an extrusion-based method using gelatin-methacryloyl bioink. *Climacteric*. 2022;25(2):170-178.

doi: 10.1080/13697137.2021.1921726

78. Yuan TY, Fu XH, Hu RC, *et al*. Bioprinted, spatially defined breast tumor microenvironment models of intratumoral heterogeneity and drug resistance. *Trends Biotechnol*. 2024;42(11):1523-1550.

doi: 10.1016/j.tibtech.2024.06.007

79. Bai LG, Hao ZY, Wang S, *et al*. Biomimetic three-dimensional glioma model printed in vitro for the studies of glioma cells and neurons interactions. *Int J Bioprint*. 2024;9(4):715.

doi: 10.18063/ijb.715

80. Jaiswal C, Dey S, Prasad J, Gupta R, Agarwala M, Mandal BB. 3D bioprinted microfluidic based osteosarcoma-on-a-chip model as a physiomimetic pre-clinical drug testing platform for anti-cancer drugs. *Biomaterials*. 2025;320:123267.

doi: 10.1016/j.biomaterials.2025.123267

81. Vítková L, Kazantseva N, Musilová L, *et al*. Magneto-responsive hyaluronan hydrogel for hyperthermia and bioprinting: magnetic, rheological properties and biocompatibility. *APL Bioeng*. 2023;7(3):036113.

doi: 10.1063/5.0147181

82. Dukov N, Bliznakova K, Okkalidis N, Teneva T, Encheva E, Bliznakov Z. Thermoplastic 3D printing technology using a single filament for producing realistic patient-derived breast models. *Phys Med Biol*. 2022;67(4):045008.

doi: 10.1088/1361-6560/ac4c30

83. Liu J, Zhao Y, Ren BH, *et al*. Multiscale vascularized tumor-on-a-chip via bioprinting for drug research. *Int J Bioprint*. 2025;11(4):378-391.

doi: 10.36922/ijb025180180

84. Wang WZ, Liu P, Zhang BQ, *et al*. Fused deposition modeling printed PLA/nano β-TCP composite bone tissue engineering scaffolds for promoting osteogenic induction function. *Int J Nanomedicine*. 2023;18:5815-5830.

doi: 10.2147/IJN.S416098

85. Gao QL, Guo ZW, Zhang SQ, *et al*. Coaxial bioprinting of microsphere bioink to engineer heterogeneous vascularized lung cancer model. *Biomater Adv*. 2026;183:214741.

doi: 10.1016/j.bioadv.2026.214741

86. Gato-Diaz U, de Castro-Alves L, Concheiro A, *et al*. Biomimetic core-shell breast cancer models using alginate, gelatin, and collagen I: simulating the tumor matrix for drug evaluation. *Int J Biol Macromol*. 2026;335:149205.

doi: 10.1016/j.ijbiomac.2025.149205

87. Jin ZZ, Li XD, Liu BX, *et al*. Coaxial bioprinted microfibers with mesenchymal stem cells for glioma microenvironment simulation. *Bio-Des Manuf*. 2022;5(2):348-357.

doi: 10.1007/s42242-021-00155-2

88. Andolfi A, Cai L, Martinez MVG, *et al*. Hyaluronic acid-based bioink for anisotropic neural tissue cryobioprinting. *Int J Extreme Manuf*. 2026;8(1):015003.

doi: 10.1088/2631-7990/adfeee

89. Chen Z, Huang CZ, Liu HL, *et al*. 3D bioprinting of complex biological structures with tunable elastic modulus and porosity using freeform reversible embedding of suspended hydrogels. *Bio-Des Manuf*. 2023;6(5):550-562.

doi: 10.1007/s42242-023-00251-5

90. Zhou KR, Rao W. Cryogenic biomanufacturing: principle, technology, and applications. *Adv Funct Mater*. 2026;36(53).

doi: 10.1002/adfm.202531265

91. Budharaju H, Kumar SKP, Rajendran M, Sivasubramanian M, Sethuraman S, Sundaramurthi D. Advances in 3D bioprinting of functional skeletal muscle constructs: focus on preclinical models and evaluation strategies. *ACS Biomater Sci Eng*. 2026;12(4):1913-1946.

doi: 10.1021/acsbiomaterials.5c01868

92. Li B, Huang C, Wang Z, *et al*. Rheology-directed design of multifunctional human-like skin materials for extrusion-based 3D bioprinting combining bioadhesion, bacteriostatic, and wound repair. *Med Eng Phys*. 2026;147(8):085003.

doi: 10.1088/1873-4030/ae8858

93. Ng WL, Shkolnikov V. Jetting-based bioprinting: process, dispense physics, and applications. *Bio-Des Manuf*. 2024;7(5):771-799.

doi: 10.1007/s42242-024-00285-3

94. Ng WL, Shkolnikov V. Optimizing cell deposition for inkjet-based bioprinting. *Int J Bioprint*. 2024;10(2):182-206.

doi: 10.36922/ijb.2135

95. Xu HQ, Liu JC, Shahriar M, Xu CX. Investigation of cell aggregation on the printing performance in inkjet-based bioprinting of cell-laden bioink. *Langmuir*. 2023;39(1):545-555.

doi: 10.1021/acs.langmuir.2c02817

96. Dell AC, Wagner G, Own J, Geibel JP. 3D bioprinting using hydrogels: cell inks and tissue engineering applications. *Pharmaceutics*. 2022;14(12):2596.

doi: 10.3390/pharmaceutics14122596

97. Wan WM, Wang X, Zhang RT, *et al*. Construction of artificial lung tissue structure with 3D-inkjet bioprinting core for pulmonary disease evaluation. *J Tissue Eng*. 2025;16.

doi: 10.1177/20417314251328128

98. Byrne R, Carrico A, Lettieri M, Rajan AK, Forster RJ, Cumba LR. Bioinks and biofabrication techniques for biosensors development: a review. *Mater Today Bio*. 2024;28:101185.

doi: 10.1016/j.mtbio.2024.101185

99. Chiticaru EA, Ionita M. Commercially available bioinks and state-of-the-art lab-made formulations for bone tissue engineering: a comprehensive review. *Mater Today Bio*. 2024;29:101341.

doi: 10.1016/j.mtbio.2024.101341

100. Xu HQ, Salazar DMM, Xu CX. Investigation of cell concentration change and cell aggregation due to cell sedimentation during inkjet-based bioprinting of cell-laden bioink. *Machines*. 2022;10(5):315.

doi: 10.3390/machines10050315

101. Lee YJ, Park JA, Tuladhar T, Jung SJE. Sonochemical degradation of gelatin methacryloyl to control viscoelasticity for inkjet bioprinting. *Macromol Biosci*. 2023;23(5).

doi: 10.1002/mabi.202200509

102. Liu JC, Shahriar M, Xu HQ, Xu CX. Cell-laden bioink circulation-assisted inkjet-based bioprinting to mitigate cell sedimentation and aggregation. *Biofabrication*. 2022;14(4):045020.

doi: 10.1088/1758-5090/ac8fb7

103. Bozek J, Kurchakova O, Michel J, *et al*. Pneumatic conveying inkjet bioprinting for the processing of living cells. *Biofabrication*. 2025;17(2):025003.

doi: 10.1088/1758-5090/ada8e2

104. Zhang JH, Wehrle E, Rubert M, Müller R. 3D bioprinting of human tissues: biofabrication, bioinks, and bioreactors. *Int J Mol Sci*. 2021;22(8):3971.

doi: 10.3390/ijms22083971

105. Choi T, Park J, Lee S, *et al*. 3D bioprinted neural tissues: emerging strategies for regeneration and disease modeling. *Pharmaceutics*. 2025;17(9):1176.

doi: 10.3390/pharmaceutics17091176

106. Rahman TT, Arman MS, Perez V, Xu B, Li JZ. Analysis of the operating conditions of pulse electric field-assisted EHD for sodium alginate printing using design of experiment approach. *Int J Adv Manuf Technol*. 2021;115(7-8):2037-2047.

doi: 10.1007/s00170-021-07042-1

107. Unagolla JM, Jayasuriya AC. Hydrogel-based 3D bioprinting: a comprehensive review on cell-laden hydrogels, bioink formulations, and future perspectives. *Appl Mater Today*. 2020;18:100479.

doi: 10.1016/j.apmt.2019.100479

108. Shulunov VR. Rapid inkjet resorbable plate scaffold 3D bioprinting technology. *Int J Artif Organs*. Published online 2026.

doi: 10.1177/03913988261471402

109. Shulunov VR, Stelmakh SA, Grigor'eva MN. Formatted water-soluble ribbon for roll porous scaffold 3D bioprinting. *Int J Artif Organs*. 2026;49(3):218-224.

doi: 10.1177/03913988261422332

110. Yadav PK, Alsaidan OA, Altemani FH, *et al*. Advancing regenerative medicine with 3D bioprinting: techniques, biomaterials, and clinical applications. *Curr Med Chem*. Published online 2026.

doi: 10.2174/0109298673445024260412125122 2

111. Campbell A, Gutierrez DA, Knight C, *et al*. Novel combinatorial strategy using thermal inkjet bioprinting, chemotherapy, and radiation on human breast cancer cells: an in-vitro cell viability assessment. *Materials (Basel)*. 2021;14(24):7864.

doi: 10.3390/ma14247864

112. Cheng C, Deneke N, Moon HR, *et al*. Inkjet-printed morphogenesis of tumor-stroma interface using bi-cellular bioinks of collagen-poly(N-isopropyl acrylamide-co-methyl methacrylate) mixture. *Mater Today Adv*. 2023;19:100408.

doi: 10.1016/j.mtadv.2023.100408

113. Krajewska U, Chechlinska M, Kurzyk A. Vascularisation in 3D bioprinted models: emerging solutions engineering functional tissues and tumour models. *Biofabrication*. 2026;18(2):022001.

doi: 10.1088/1758-5090/ae2f02

114. Liu X, Xu M, Wang H, Zhu L. Bioprinting strategies for skeletal muscle regeneration: advances in bioinks, technologies, and functional reconstruction. *Int J Bioprint*. 2025;11(5):46.

doi: 10.36922/ijb025300306

115. Narayanan KB. Advances in 3D bioprinting for scaffold-based and scaffold-free tissue engineering and regenerative medicine. *Gels*. 2026;12(8):691.

doi: 10.3390/gels12080691

116. Narayanan KB, Han SS. 3D bioprinting modalities for tissue engineering and regenerative medicine. *Adv Colloid Interface Sci*. 2026;358:104026.

doi: 10.1016/j.cis.2026.104026

117. Le NN, Phan HCT, Dang DMT, Dang CM. Fabrication of miniaturized microfluidic paper-based analytical devices for sandwich enzyme-linked immunosorbent assays using inkjet printing. *Appl Biochem Microbiol*. 2021;57(2):257-261.

doi: 10.1134/S0003683821020071

118. Mea H, Wan J. Microfluidics-enabled functional 3D printing. *Biomicrofluidics*. 2022;16(2):021501.

doi: 10.1063/5.0083673

119. Cheah E, Gao XC, Jaw WQ, *et al*. Customizable fabrication of 2D and conformal multielectrode arrays for 3D printed organotypic bioelectronic interfaces. *Adv Healthc Mater*. 2026;15(8):e02757.

doi: 10.1002/adhm.202502757

120. Gibney R, Ferraris E. Bioprinting of collagen type I and II via aerosol jet printing for the replication of dense collagenous tissues. *Front Bioeng Biotechnol*. 2021;9:786945.

doi: 10.3389/fbioe.2021.786945

121. Williams NX, Watson N, Joh DY, Chilkoti A, Franklin AD. Aerosol jet printing of biological inks by ultrasonic delivery. *Biofabrication*. 2020;12(2):025004.

doi: 10.1088/1758-5090/ab5cf5

122. Han Z, Huang J, Qiu X. Advances and challenges in 3D bioprinting of cartilage organoids: from material innovation to functional regeneration. *Int J Nanomedicine*. 2026;21(2):1-24.

doi: 10.2147/IJN.S518179

123. Varma PY, Diksha S, Sonar VA, *et al*. Polymer materials for additive manufacturing: a comprehensive review of selection, processing, and emerging applications. *Polym Plast Technol Mater*. 2026;65(15):1609-1646.

doi: 10.1080/25740881.2026.2714219

124. Gonzalez G, Roppolo I, Pirri CF, Chiappone A. Current and emerging trends in polymeric 3D printed microfluidic devices. *Addit Manuf*. 2022;55:102867.

doi: 10.1016/j.addma.2022.102867

125. Mehta V, Rath SN. 3D printed microfluidic devices: a review focused on four fundamental manufacturing approaches and implications on the field of healthcare. *Bio-Des Manuf*. 2021;4(2):311-343.

doi: 10.1007/s42242-020-00112-5

126. Ghazali HS, Askari E, Ghazali ZS, Naghib SM, Braschler T. Lithography-based 3D printed hydrogels: from bioresin designing to biomedical application. *Colloid Interface Sci Commun*. 2022;50:100667.

doi: 10.1016/j.colcom.2022.100667

127. Liang RJ, Gu YQ, Wu YC, Bunpetch V, Zhang SF. Lithography-based 3D bioprinting and bioinks for bone repair and regeneration. *ACS Biomater Sci Eng*. 2021;7(3):806-816.

doi: 10.1021/acsbiomaterials.9b01818

128. Lim KS, Galarraga JH, Cui XL, Lindberg GCJ, Burdick JA, Woodfield TBF. Fundamentals and applications of photo-cross-linking in bioprinting. *Chem Rev*. 2020;120(19):10637-10669.

doi: 10.1021/acs.chemrev.9b00812

129. Prados-Martin L, Tran HA, Mota C, *et al*. Advances in light-based 3D bioprinting. *Biofabrication*. 2026;18(3):033001.

doi: 10.1088/1758-5090/ae7208

130. Schwab A, Levato R, D'Este M, Piluso S, Eglin D, Malda J. Printability and shape fidelity of bioinks in 3D bioprinting. *Chem Rev*. 2020;120(19):10850-10877.

doi: 10.1021/acs.chemrev.0c00084

131. Azzariti LL, Muir VG. Dynamic covalent hydrogels for bioprinting and soft material additive manufacturing. *ACS Appl Polym Mater*. 2026;8(15):12141-12163.

doi: 10.1021/acsapm.6c01725

132. Rani S, Das RK, Suryawanshi T, *et al*. Directed cell growth of C2C12 cells on ECM free bioprinted nano/micro scaffolds. *Small*. 2025;21(4):2405928.

doi: 10.1002/smll.202405928

133. Choi Y, Kim SJ, Park JK. Configurable 3D-printed microstructured stamp as a user-friendly tool for versatile

patterning of low-viscosity bioinks. *Adv Mater Technol*. 2025;10(22):e00442.

doi: 10.1002/admt.202500442

134. Chen S, Cao J, Ye X, *et al*. Limbal organoids and bioengineering sheets based on niche microphysiological systems and bioprinting for corneal injury repair in rabbits. *Acta Biomater*. 2026;216:137-155.

doi: 10.1016/j.actbio.2026.04.042

135. Fournié V, Venzac B, Trevisiol E, *et al*. A microfluidics-assisted photopolymerization method for high-resolution multimaterial 3D printing. *Addit Manuf*. 2023;72:103629.

doi: 10.1016/j.addma.2023.103629

136. Lee S, Kim JH, Kang SJ, Chang IH, Park JY. Customized multilayered tissue-on-a-chip (MToC) to simulate Bacillus Calmette-Guerin (BCG) immunotherapy for bladder cancer treatment. *Biochip J*. 2022;16(1):67-81.

doi: 10.1007/s13206-022-00047-2

137. Soliman BG, Major GS, Atienza-Roca P, *et al*. Development and characterization of gelatin-norbornene bioink to understand the interplay between physical architecture and micro-capillary formation in biofabricated vascularized constructs. *Adv Healthc Mater*. 2022;11(2):2101873.

doi: 10.1002/adhm.202101873

138. Dong YX, Qian SY, Wang XC, *et al*. In situ tailored confining microenvironment for lung cancer spheroids. *Mater Today Bio*. 2025;31:101602.

doi: 10.1016/j.mtbio.2025.101602

139. Gan Q, Ge ZX, Wang XD, *et al*. Stiffness-tunable substrate fabrication by DMD-based optical projection lithography for cancer cell invasion studies. *IEEE Trans Biomed Eng*. 2024;71(7):2201-2210.

doi: 10.1109/TBME.2024.3364971

140. Dzikonski D, Bekker E, Zamboni R, *et al*. Hybrid microfluidic chip design with two-photon polymerized protein-based hydrogel microstructures for single cell experiments. *Adv Mater Technol*. 2025;10(9):2401571.

doi: 10.1002/admt.202401571

141. He ZY, Cheng PP, Ying GQ, Ou ZM. Research progress in the construction and application of in vitro vascular models. *Appl Sci (Basel)*. 2024;14(15):6780.

doi: 10.3390/app14156780

142. Salerno A, Netti PA. Review on computer-aided design and manufacturing of drug delivery scaffolds for cell guidance and tissue regeneration. *Front Bioeng Biotechnol*. 2021;9:682133.

doi: 10.3389/fbioe.2021.682133

143. Breideband L, Wächtershäuser KN, Hafa L, *et al*. Upgrading a consumer stereolithographic 3D printer to produce a physiologically relevant model with human liver cancer organoids. *Adv Mater Technol*. 2022;7(10):2200029.

doi: 10.1002/admt.202200029

144. Li YE, Xing HY, Lai L, *et al*. Additive manufacturing of graphene oxide-doped SiOC/Si3N4 photothermal functional bioceramic scaffolds through stereolithography technology. *J Adv Ceram*. 2025;14(7):9221098.

doi: 10.26599/JAC.2025.9221098

145. Gretser S, Kinzler MN, Theilen TM, Wild PJ, Vogler M, Gradhand E. Fluorescence confocal microscopy for evaluation of fresh surgical specimens and consecutive tumor cell isolation in rare pediatric tumors. *Virchows Arch*. 2025;486(3):585-593.

doi: 10.1007/s00428-024-03861-1

146. Han C, Zhang RC, He XW, *et al*. A digital manufactured microfluidic platform for flexible construction of 3D co-culture tumor model with spatiotemporal resolution. *Biofabrication*. 2025;17(1):015029.

doi: 10.1088/1758-5090/ad9636

147. Barin N, Chowdhury SZ, de Wit M, *et al*. Two-photon polymerized microvascular environments for multicellular modeling of the blood-brain tumor barrier. *Adv Mater Technol*. 2026.

doi: 10.1002/admt.202502614

148. Genchi GG, Conci C, Sen Ö, *et al*. Two-photon polymerization of miniaturized 3D scaffolds optimized for studies on glioblastoma multiforme in spaceflight-like microgravity conditions. *Biofabrication*. 2025;17(2):025024.

doi: 10.1088/1758-5090/adbb21

149. Xiao XY, Cai H, Huang QR, *et al*. Polymeric dual-modal imaging nanoprobe with two-photon aggregation-induced emission for fluorescence imaging and gadolinium-chelation for magnetic resonance imaging. *Bioact Mater*. 2023;19:538-549.

doi: 10.1016/j.bioactmat.2022.04.026

150. Guzzi EA, Bischof R, Dranseikiene D, *et al*. Hierarchical biomaterials via photopatterning-enhanced direct ink writing. *Biofabrication*. 2021;13(4):044105.

doi: 10.1088/1758-5090/ac212f

151. Sailer A, Meiring JCM, Heise C, *et al*. Pyrrole hemithioindigo antimitotics with near-quantitative bidirectional photoswitching that photocontrol cellular microtubule dynamics with single-cell precision. *Angew Chem Int Ed Engl*. 2021;60(44):23695-23704.

doi: 10.1002/anie.202104794

152. Yu C, Miller KL, Schimelman J, *et al*. A sequential 3D bioprinting and orthogonal bioconjugation approach for precision tissue engineering. *Biomaterials*. 2020;258:120294.

doi: 10.1016/j.biomaterials.2020.120294

153. Huang YH, Ono A, Sudo R. Advances in in vitro vascularization of engineered tissues: from microvessel formation to hepatic tissue integration. *Regen Ther*. 2026;32:101086.

doi: 10.1016/j.reth.2026.101086

154. Vidler C, Halwes M, Collins DJ. In situ characterisation of hydrogels via dynamic interface printing. *Adv Sci (Weinh)*. 2026.

doi: 10.1002/advs.202515106

155. Shashikumar U, Saraswat A, Deshmukh K, *et al*. Innovative technologies for the fabrication of 3D/4D smart hydrogels and its biomedical applications—a comprehensive review. *Adv Colloid Interface Sci*. 2024;328:103163.

doi: 10.1016/j.cis.2024.103163

156. Cui XR, Liu DD, Lu X, *et al*. Advanced dECM-based bioprinting strategy for tissue regeneration. *Mater Today Adv*. 2026;29:100733.

doi: 10.1016/j.mtadv.2026.100733

157. Liu Q, Ran B, Li M, Xu Q, Cui X, Xu W. Advanced 3D bioprinting of cell-laden bioinks for cartilage and osteochondral repair. *Mater Today Adv*. 2026;31:100930.

doi: 10.1016/j.mtadv.2026.100930